NRC Research Press

ARTICLE

Tunnel behaviour associated with the weak Alpine rock masses of the Driskos Twin Tunnel system, Egnatia Odos Highway

N. Vlachopoulos, M.S. Diederichs, V. Marinos, and P. Marinos

Abstract: Based on the excessive deformations and support failure encountered during tunnel construction at the Driskos Twin Tunnel site in Northern Greece, this paper provides insight on how tunnels designed in such weak rock environments can be realistically analyzed with a view of determining better analytical tools to predict deformations and improving current design methods. Specific factors that were assessed include rock strength based on the geological strength index (GSI), tunnel deformation, numerical analysis techniques employed, three-dimensional model type, support considerations, dilation, sequencing of tunnel excavation, influence of single bore construction on twin bore, and homogenization of tunnel faces. This work involves the use of nominally identical two- and three-dimensional numerical models of tunnel sequencing for analytical simulation of weak material behaviour and sequential tunnel deformation response with the goal of investigating the strength and deformation of such weak rock masses. These have been used in combination with monitoring data that were obtained in the field during the Driskos Twin Tunnel construction. A discussion of the geological conditions, material property determination, monitoring data, and model calibration strategy is given. This paper provides insight into these issues and poses many more fundamental questions regarding the analysis of tunnel excavation within weak rock masses requiring further investigation.

Key words: weak rock masses, tunnel convergence, linear displacement profile (LDP), two- and three-dimensional numerical modelling techniques for tunnelling.

Résumé : Cet article présente des informations sur comment la conception de tunnels dans des environnements de roches peu résistantes peut être analysée de façon réaliste, dans le but de déterminer les meilleurs outils analytiques de prédiction des déformations et d'améliorer les méthodes de conception actuelles, et ce, à partir du cas du tunnel double de Driskos au nord de la Grèce, où des déformations excessives et une rupture de support ont été observées durant la construction. Les facteurs spécifiques évalués incluent : la résistance de la roche selon l'indice de résistance géologique (IRG), la déformation du tunnel, les techniques d'analyse numérique utilisées, le type de modèle à trois dimensions, les considérations de support, la dilatation, la séquence d'excavation du tunnel, l'influence de la construction à un forage sur le forage double et l'homogénéisation des faces du tunnel. Ce travail implique l'utilisation de modèles numériques à deux et à trois dimensions à peu près identiques de la séquence construction pour simuler analytiquement le comportement des matériaux peu résistants et la réponse en déformation séquentielle du tunnel, afin d'étudier la résistance et déformation de ce type de masse rocheuse peu résistante. Ces modèles ont été utilisés en combinaison avec des données de suivi obtenues sur le terrain durant la construction du tunnel double de Driskos. Une discussion des conditions géologiques, de la détermination des propriétés des matériaux, des données de suivi et du calibrage du modèle est présentée. Cet article propose une meilleure compréhension sur ces sujets et pose plusieurs autres questions fondamentales en lien avec l'analyse de l'excavation d'un tunnel à travers des masses rocheuses peu résistantes, qui demandent des investigations supplémentaires. [Traduit par la Rédaction]

Mots-clés : masses rocheuses peu résistantes, convergence du tunnel, profil de déplacement linéaire (PDL), techniques de modélisation numériques à deux et à trois dimensions pour les tunnels.

Introduction

Current practice in designing temporary support for tunnel construction in weak rock masses is contingent on a suitable assessment of the rock mass (quality and strength) that is to be encountered throughout the tunnel alignment. The most widely used criteria for estimating rock mass properties is that presented by Hoek and Marinos (2002*a*). In tunnelling through weak heterogeneous rock masses such as those of flysch, it is important to obtain reliable strength estimates of rock materials to predict potential tunnelling problems as early as possible in the design process. This is a nontrivial undertaking.

A rock mass classification system framework is also required. The geological strength index (GSI) was used for this investigation (Marinos and Hoek 2000). This classification system allows the estimation of the rock mass properties in varying geological conditions. The main criteria associated with the GSI classification system is a detailed engineering geology description of the rock mass that is qualitative in nature. This grew out of the notion that numbers on joints were largely meaningless for weak and complex rock masses (Marinos et al. 2006). This index is based upon an assessment of the structure, lithology, and condition of discontinuity surfaces in the rock mass. The GSI value of a rock mass is incorporated into calculations to determine the reduction in the strength and modulus of the rock mass as compared with the strength and modulus of the intact rock components. An interpretation of GSI (or the applicability of the system itself) for a particular rock mass may vary significantly amongst geologists

Received 18 January 2012. Accepted 22 May 2012.

N. Vlachopoulos and M.S. Diederichs. Geo-Engineering Centre Queen's University–Royal Military College of Canada, Kingston, ON K7L 3N6, Canada.
V. Marinos. Department of Geology, Faculty of Sciences, Aristotle University of Thessaloniki, GR-541 24 Thessaloniki, Greece.
P. Marinos. School of Civil Engineering Geotechnical Dept. 9, National Technical University of Athens, Iroon Polytechniou str., 157 80 Zografou, Athens, Greece.
Corresponding author: Nicholas Vlachopoulos (e-mail: vlachopoulos-n@rmc.ca).

and tunnel designers if its geological description is not interpreted in the same manner.

As well, an assessment of the size of the final plastic zone around a tunnel cavity and its ensuing influence on tunnel deformations has only recently been incorporated into industry-standard, two-dimensional (2D) design analysis (Vlachopoulos and Diederichs 2009). Observational design methods have been applied successfully to difficult tunnel conditions (Marinos et al. 2007); however, these are usually applied only after excessive deformations have been observed in the field.

The backdrop for this research paper is based on the tunnelling that has recently been completed in the Epirus and Western Macedonia regions of Northern Greece, as part of the massive Egnatia Odos Highway construction project. Due to the difficult geological conditions and weak rock masses that were encountered during the construction of the 4.5 km long Driskos Twin Tunnel, excessive deformations and temporary support failures were experienced at various sections of the tunnel alignment during tunnel production. In this way, the Driskos Twin Tunnel project provides an excellent case study for analyzing excessive tunnel deformations within weak rock masses. Accurate equivalent rock mass performance predictions for tunnels in such materials (including yield and residual strength as well as flow and dilation considerations) are complicated by other structural peculiarities (mixed face conditions, anisotropy due to the structural elements).

Case study: Driskos Twin Tunnel, Egnatia Odos Highway, Greece

The 670 km long Egnatia Odos Highway is a massive construction project completed recently in Northern Greece to open up new, modern, and safe roads connecting the countries of the European Union, the Balkans, and the Middle East. The highway includes 77 twin tunnels and over 600 bridges along the alignment. The motorway was designed to the specifications of the Trans-European network. Due to the geological setting, many geotechnically unfavourable characteristics were encountered within the Egnatia Odos Highway alignment. The great variety of geological–geotechnical situations imposed the need for different approaches in designing the various components of the highway (Hoek and Marinos 2006). A geotechnical rock mass model had to be defined to choose the appropriate geotechnical parameters for the design of cuts, embankments, and tunnels. The next section will outline the main geological conditions that were encountered during construction at the Driskos Twin Tunnel site and introduce the main geotechnical and rock mass assessment framework that was utilized for this project.

Geological environment

The overall geology of Greece and that of the Alpine region has traditionally been described in terms of isopic zones and massifs. These zones are groups of widespread rocks that have shared a common history, both in the ancient environments of deposition of sediments and their faulting and folding. The massifs of metamorphic and plutonic rocks are more resistant to folding and faulting than adjacent sediments. Heterogeneous rock masses such as flysch (a tectonically reworked clastic mix) are also abundant. Greece's geology is still very active as it is located on a converging plate rim between the European and African plate. Figure 1 summarizes the "isopic" zones and significant structural elements.

The Egnatia Odos Highway traverses the entire width of Greece, crossing almost perpendicularly all the main geotectonic units. Each zone presents unique engineering geology challenges for construction and tunnelling and these have been summarized by Hoek and Marinos 2006 and Vlachopoulos and Diederichs 2009. Figure 2 depicts the typical topography within NorthWestern Greece showing tunnelling works that are part of the Egnatia Odos Highway.

Fig. 1. Map of the External Hellenides showing the "isopic" zones and significant structural elements (modified after Doutsos et al. 2006).

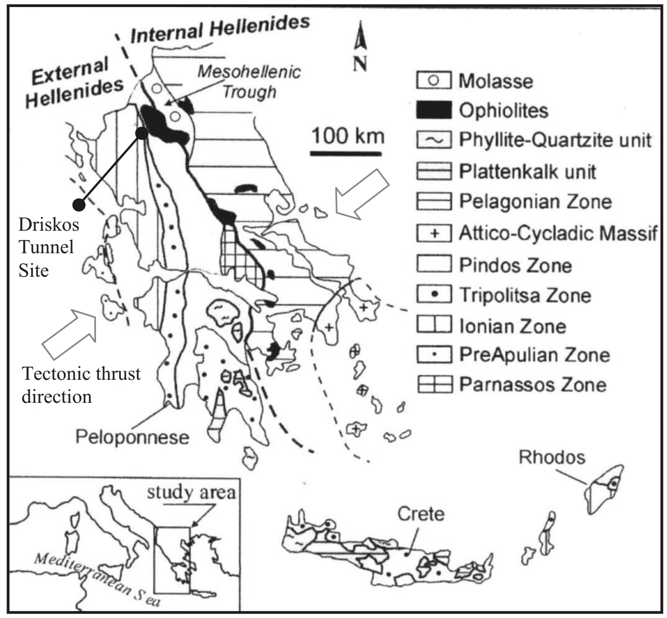

Fig. 2. Portals of tunnels of Egnatia Odos Highway depicting the nature of the challenging geological conditions.

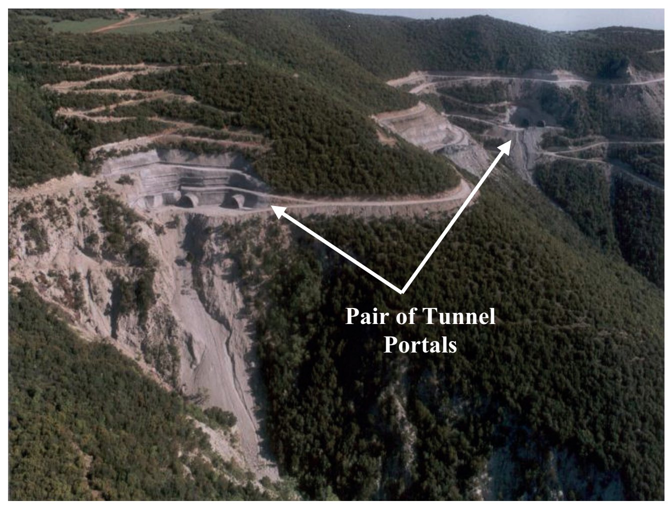

The Driskos Twin Tunnel is situated in a series of varying lithological features of the Ionian tectonic unit adjacent to the Pindos isopic unit (Fig. 1). The material is less tectonically disturbed than the Pindos flysch and therefore, there is an absence of extensive chaotic zones within the Ionian flysch. The primary rock mass material consists of flysch, which consists of varying alterations of clastic sediments that are associated with orogenesis. It closes the cycle of sedimentation of a basin before the "arrival" of the paroxysm folding process. The clastic material derives from erosion of the previously formed neighbouring mountain range. Flysch is characterized by rhythmic alterations of sandstone and fine-grained (politic) layers. The sandstone may also include conglomerate beds. More geological and strength characteristics associated with flysch are contained in Marinos and Hoek (2001).

The main lithological formations that were encountered during the excavation of the Driskos Twin Tunnel are as follows (data from Egnatia Odos, S.A. 2003 and Marinos 2007):

Fig. 3. (*a*) Examples of thin-bedded alternations of siltstones and sandstones from Mt. Driskos region (folding of the formations is evident in part (*c*)). (*b*) Medium- to thick-bedded sandstones and thin-bedded siltstones; shear zones exist along the bedding planes and the fracturing (faults) along axial plains. (*c*) Thick-bedded sandstones with alternations of thin-bedded siltstones.

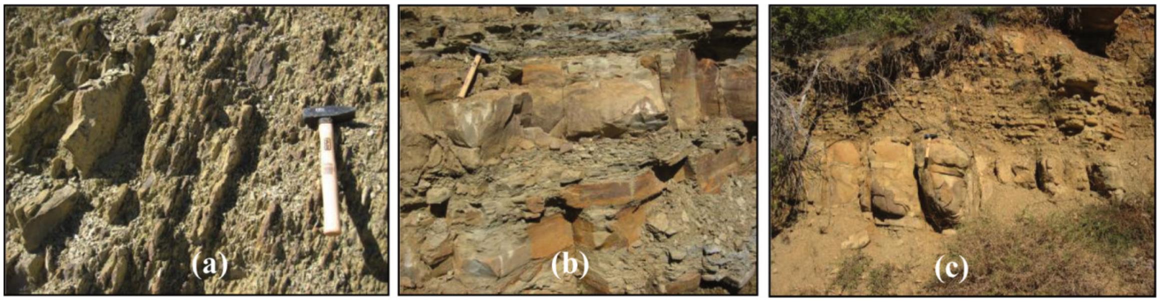

Fig. 4. Longitudinal topographic profile and idealized cross section of Driskos Twin Tunnel alignment depicting the rock formations that have been traversed (modified after Egnatia Odos, S.A. 2003 and Hoek and Marinos 2000*b*).

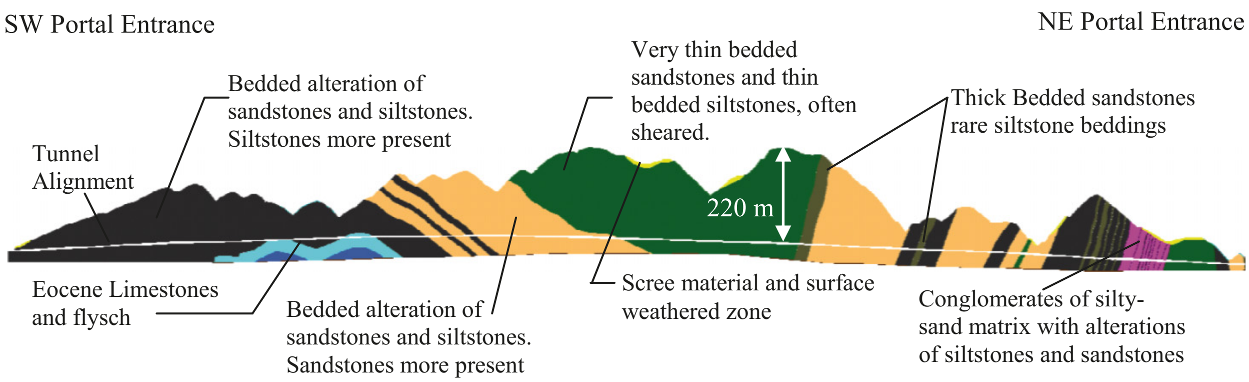

1. Siltstones with thinly bedded sandstones (10 cm) (Si).
2. Thin- to medium-bedded alternations of siltstones and sandstones (SiSa).
3. Medium- to thick-bedded sandstones with interbedded siltstones (SaSi).
4. Thick-bedded sandstones with alternations of thin-bedded siltstones (Sa).
5. Conglomerates (Fc/SiSa).

Selected examples of these rock masses are shown in Fig. 3. To more effectively study the various formations and rock masses that were encountered by the Driskos Twin Tunnel alignment, a geological Driskos longitudinal section was prepared (Fig. 4).

Rock mass type and parameters

In tunnelling through weak heterogeneous rock masses such as those found in Greece, it is important to obtain reliable strength estimates of this material to predict potential tunnelling problems as early as possible in the design process. These parameters must be incorporated into an overall rock mass criteria framework (i.e., Hoek–Brown rock mass characterization tool), which are also part of a well-defined rock mass characterization system (i.e., GSI for weak heterogeneous rock masses).

Currently, the most widely used criteria for estimating rock mass properties is that presented by Hoek and Brown (1997), and updated by Hoek et al. (2002) and Hoek and Diederichs (2006) (for rock modulus of elasticity). This generalized Hoek–Brown criterion for intact rock samples approximates the nonlinear relationship between maximum axial stress, σ_1, that can be sustained by the sample and the applied confining stress, σ_3. In its generalized form, the following parabolic law defines this relationship:

$$[1] \qquad \sigma_1' = \sigma_3' + \sigma_{ci}\left(m_b\frac{\sigma_3'}{\sigma_{ci}} + s\right)^a$$

where σ_1' and σ_3' are the maximum and minimum effective stresses at failure, respectively, σ_{ci} is the uniaxial compressive strength of the intact rock pieces, m_b (or m_i for intact strength) is a Hoek–Brown constant and a parameter deduced from σ_1' and σ_3' test results of a particular rock type. Constants *s* and *a* are unique to the rock mass and are based upon the specific rock mass characteristics.

The Hoek–Brown criterion was the primary characterization tool used for this investigation. As mentioned above, three parameters are required to estimate the strength and deformation properties: the uniaxial compressive strength (σ_{ci}) of the "intact" rock elements; a constant, *m*, that defines the frictional characteristics of the rock; and the GSI. The GSI was introduced by Hoek et al. (1995) and Hoek and Brown (1997), and extended by Hoek et al. (1998) and Marinos et. al. (2007). The GSI is based upon an assessment of the structure, lithology, and condition of discontinuity surfaces in the rock mass, and is estimated through visual examination of the rock mass exposed in tunnel faces. The GSI value of a rock mass is incorporated into calculations to determine the reduction in the strength of the rock mass as compared with the strength of the intact rock components. This GSI method was deemed as an appropriate tool for evaluating closely jointed rock masses.

Marinos and Hoek (2000) also developed a GSI table specifically for heterogeneous rock masses such as flysch. Marinos (2007, 2010) also updated the GSI table for Flysch material, but this assessment was not available at the design stage of the Driskos Twin Tunnel and is not used within this research investigation. Based on these strength values, categories of the rock mass were determined.

Fig. 5. Schematic summary section of major geological units crossing the Driskos Twin Tunnel alignment at depth. Geomechanical properties averaged over lengths shown. Numbered zones represent unique engineering geology.

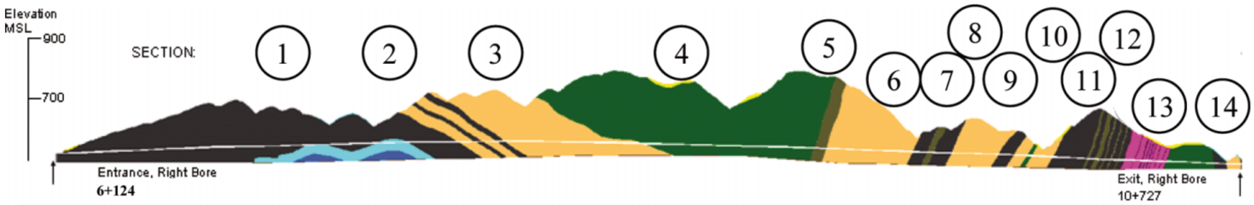

Chaînage Silt(Si)-Sand(Sa)-Stone	6+124 – 6+248	Sisa 7+625	SaSi/ Sisa 7+840	SaSi 8+385	**Sisa/ Si+SaSi** 9+035	Sa-An 9+085	SaSi 9+425	Sa+SiSa 9+580	SaSi/SiSa+Si 9+975	SiSa 10+105	Sa+SiSa 10+260	Fa/SiSa 10+420	Si/SiSa 10+610	SaSi/Sa+SiSa 10+727
GSI average	35-40	35-50	40~50	50-65	**30-35**	60~65	50-60	45~60	45-65	45-50	25~50	35-45	25~50	45~50
Rock-mass Elastic Modulus E (GPa)	HCC = 1.3 - 1.8 HD = 0.4 - 0.6	*Hoek,Carranza-Torres & Corkum 2002 *HCC = 2.1 - 5.5 **HD = 1.1 – 3.5 ** Hoek & Diederichs 2006 (MR=400)	HCC = 3.1 – 6.7 HD = 1.9 – 5.5	HCC = 6.7 - 18 HD = 5.9 - 16	**HCC = 1 - 2.3** **HD = 0.33 - 1.4**	HCC = 9.7 - 15 HD = 5.9 - 9.5	HCC = 6.7 - 14 HD = 5.9 - 13	HCC = 4.1 – 11 HD = 2.5 - 7.8	HCC = 3.3 - 15 HD = 1.8 - 10	HCC = 4.1 - 5.5 HD = 2.5 - 3.5	HCC = 0.75 - 5.5 HD = 0.23 – 3.5	HCC = 1.6 - 3.8 HD = 0.64 – 2.1	HCC = 0.67 - 3.9 HD = 0.2 - 1.8	HCC = 4.7 - 6.7 HD = 3.6 - 5.5
Mi (est)	10	10	12	14	**11**	12	10	15	12	14	15	14	10	13
Strength (MPa) UCS = intact RM = rockmass	UCS = 10 RM = 0.9 –1.1	UCS 25 – 30 ^RM 2.4 – 4.7 ^Hoek,Carranza-Torres & Corkum 2002	UCS = 30 - 45 RM = 3.1 – 6.7	UCS = 45-60 RM = 6.3 – 14.7	**UCS = 10 – 30** **RM = 0.7 – 2.5**	UCS = 30 – 40 RM = 6.4 – 10.2	UCS = 45-60 RM =6.3 – 12.2	UCS = 30 – 40 RM = 4.1 – 9.1	UCS = 20-40 RM =2.3-9.8	UCS = 30 RM = 4-4.7	UCS = 10-30 RM = 0.7-4.9	UCS = 15 - 25 RM = 1.4– 3.2	UCS = 8-15 RM 0.4-2.1	UCS = 40-45 RM = 5.2-6.9

Figure 5 shows the 14 sections (as divided by the authors) associated with the Driskos Twin Tunnel site and relevant material properties related to each of these sections. Chainage values are also included in this figure. These values correspond with the original geodetic investigation by Egnatia Odos, S.A. (1998) and have been used here for ease of reference and cross-referencing purposes. The Driskos Twin Tunnel alignment begins to the west at a chainage of 6 + 124 (entrance) (i.e., at kilometre 6 within this region of the Egnatia Odos Highway construction works; at 124 m in). The southwest (SW) tunnel portal begins and continues to 10 + 727, the mark for the northwest (NW) tunnel portal exit.

Also conducted within the Driskos Twin Tunnel alignment was a site investigation that included 18 boreholes over the 4.5 km tunnel alignment. Selected engineering strength properties from these borehole samples as well as samples collected from outcrops in the area are included in Tables 1 to 4. A GSI range of 25–38 and a modulus of elasticity (E_{rm}) of 1400 MPa encompass most of the problematic geological sections encountered during the construction of the Driskos Twin Tunnel. The overburden (in situ) stress and the strength values of the rock mass assessment predicted that the region with the most squeezing potential (i.e., largest expected strain) would be located between the 8 and 9 km chainage marks (i.e., the section labeled 4 within Fig. 5). The section was estimated by the methodology described by Hoek and Marinos 2000*a*. This is seen in Fig. 6.

Tunnel design and construction

General

The material through which the Driskos Twin Tunnel was bored cannot be fully defined in terms of well-known strength and deformation properties as identified in the previous section (i.e., materials are often discontinuous, inhomogeneous, and anisotropic in nature). A design must take into consideration the effects of the disturbance caused by tunnel excavation including stages of excavation not completely confined by the long-term support and final lining. It is during this stage that the pre-existing stresses in the rock mass (deviated by the opening of the tunnel) are channelled around the cavity in an arch effect, creating zones of increased stress on the walls of the excavation. The most important task of a tunnel design engineer is to determine

Table 1. Design values of the uniaxial compressive strength, of intact rock, and of the tensile strength for every rock mass category (II–V) and lithology (modified after from Egnatia Odos, S.A. 2003).

	Compressive strength, σ_{ci} (MPa)				Tensile strength, σ_t (MPa)			
Lithology	II	III	IV	V	II	III	IV	V
Sa	80	60	40	—	8	6	4	—
SaSi	60	45	30	—	5.5	4.5	3.5	—
SiSa	35	30	25	10	4	3	2	—
Si	10	10	8	7	2	1	0	0
Fc	25	20	15	—	2	1	0	0

Table 2. Uniaxial compressive strength of sandstone and siltstone as determined for Driskos (data from Egnatia Odos, S.A. 2003).

Rock Type or Formation	Designation	Uniaxial compressive strength, σ_c (MPa)	Friction angle, ϕ (°)
Sandstone	Sa	40–80	30–35
Predominant sandstone with alternations of siltstone	SaSi	30–60	—
Predominant siltstone with alternations of sandstone	SiSa	10–35	—
Siltstone	Si	7–10	27–30

Table 3. Engineering material parameters associated with relevant rock mass quality categories as determined prior to excavation for Driskos (modified after from Egnatia Odos, S.A. 2003). Unit weight of rock mass, γ, is 27 kN/m³ in all cases shown.

Rock mass quality category	Rock type/ formation	GSI	σ_{ci} (MPa)	m_i	σ_{cm}	Modulus, E (MPa)	Overburden (m)	In situ stress, p_o (MPa)
III	Si	40	10	9	0.86	1590	100	2.7
IV	Si	40	10	9	0.86	1590	150	4.05
Va	SiSa/Si+SaSi	25	15	11	1.02	918	150	4.05
Vb	SiSa/Si+SaSi	25	15	11	1.09	887	220	5.94

Table 4. Borehole (BH) locations by chainage and relevant strength and depth information (data from Egnatia Odos, S.A. 2003).

Borehole	Chainage	GSI	Rock mass quality category	Depth of borehole (m)
BH-15	6+601	58–60	III	115.0
BH-13	6+651	52–54	III	115.0
BH-9	7+301	45–49	III	65.0
BH-16	7+901	55–57	III–IV	110.0
BH-10	8+501	42–44	IV	195.0
BH-17	8+709	43	III	135.9
BH-11	8+812	42–44	IV	175.0
BH-12	9+451	57–59	III	75.1
BH-4	9+907	49–51	III	50.2
BH-6	10+551	50–59	III	95.0
BH-7	10+621	59–62	III	30.0
	7+900–8+460	57–68	II–III	—
	9+160–9+500	57–68	II–III	—
	8+460–9+110	30–37	IV–V	—
	9+110–9+160	64–73	II	—

how and if an arch effect can be triggered when a tunnel is excavated. The engineer must then ensure that the arch effect is formed by calibrating excavation and stabilization operations (Lunardi 2000). Understanding this rock mass and support interaction becomes a critical issue.

The purpose of tunnel support is to maintain confinement for the rock mass to help the rock mass support itself. Under these confined conditions, the interlocking components of the rock pieces produce a strong and stable rock mass. Care must be taken when excavating the face to ensure that confined conditions can be maintained. This is achieved through the immediate installation of support technologies, such as (not the same in all cases) fibreglass dowels, spiles, shotcrete, rock bolts, and grouting. Again, the initial support systems installed at or in advance of the tunnel face serve to retain the rock mass integrity and provide all of the short-term support and permit the ultimate installation of the final lining. Excavation in most tunnels within a weak rock mass is carried out in this staged fashion. A top heading can be excavated and then a bench (or invert sections) may be left in place for further support. The primary support comes from the initial installation of rock bolts and steel arched rib sections supplemented with shotcrete (Fig. 7).

A typical approach would involve the development of a number of typical cross sections for support design. Each section would be related to an anticipated magnitude of strain (or radial displacement). When advancing through difficult ground the use of the forepoling umbrella arch method is often employed. For a 10 m span of tunnel, this method would typically involve the installation of 12 m long, 75 to 110 mm (or longer) diameter grouted pipe forepoles at a spacing of 300 to 600 mm. The forepoles are installed every 8 m to provide a minimum overlap of 4 m between successive umbrellas. This method is used in combination with other support systems such as steel sets embedded in shotcrete. Face stabilization by grouted fibreglass dowels and the use of a temporary invert (bench) to control floor heave are used in very weak conditions (Hoek 1999; refer to Fig. 7).

Design and construction of Driskos Twin Tunnel

The tunnel construction at the Driskos site consists of twin, parallel tunnels that are approximately 4570 m in length with a maximum overburden of 220 m. The cross section's alignment is shown in Fig. 5. In a generic sense, the geological profile shows a gently folded synclinal structure at the centre of the alignment, which elevates to an anticline at the southern end. The Driskos Twin Tunnel is, on average, 850 m above mean sea level and excavation began in 1999 with excavation being driven from both ends. The faces were split into a 60 m² top heading followed by a 40 m² bench. The tunnels were advanced using a Tamrock Para 206 T two-boom and basket drill rig. The north portals were constructed using an umbrella canopy for 50 m followed by 40–50 m cut and cover with another 20–30 m of forepole umbrella (Smith 2000).

Cross passages connecting the two tunnels occur every 350–400 m. A 180 m ventilation shaft was also constructed near the centre of the tunnel alignment. Tunnel separation is at most 18.2 m between each bore. In terms of tunnel bore dimensions, a single bore cross section has dimensions of 9.47 m by 11.0 m with respect to rock mass excavation tolerances. The cross sections of the bores are arranged in a horseshoe configuration. An idealized cross section of this nature can be seen in Fig. 8.

Support categories

As described by Marinos and Hoek (2000), a function of stress, strain, and rock mass quality (i.e., tunnel deformation / tunnel diameter versus rock mass strength / in situ stress) defines the support requirements for tunnel excavations through rock at a specific site. Further, they went on to describe the various support methods for temporary support of tunnels within weak rock masses. This exercise was no different for the site-specific design associated with the twin tunnels as part of the Driskos Twin Tunnel. The main factors that influenced the design were lithology, rock mass quality, and the height of overburden (i.e., in situ stress). Based on these results, four rock mass categories (categories II–V, with II being the better rock mass in terms of strength) and corresponding support categories (Fig. 9) were defined (Structural Design, S.A. 1999; Egnatia Odos, S.A. 2003;). The percentage of rock masses and support systems corresponding to the overall carriage length for the Driskos Twin Tunnel is

Category II – 22%	Trends:
Category III – 42%	Deteriorating rock mass strength
Category IV – 27%	Increased support requirements
Category V – 8%	

Shown in Fig. 9 are the extent of support measures that were incorporated in the preliminary design for the Driskos Twin Tunnel. One can see the increased mechanical support requirements from category II through to category V. Included within the support requirements are rockbolts, shotcrete, steel-sets, and forepoles.

The support measures that correspond to the rock mass categories for the Driskos Twin Tunnel are summarized in Table 5. Category V was further sub-divided into Va and Vb based on the

Fig. 6. Analysis of potential large-strain, squeezing regions along the Driskos Twin Tunnel alignment, based on the strength of the rock mass and the depth of overburden: (*a*) graph of overburden versus chainage along the Driskos Twin Tunnel alignment, (*b*) graph of the calculated percentage strain along the tunnel, and (*c*) photos depicting cited observations within problematic area; spalling of the shotcrete surrounding a highly stressed lattice girder and deformed rockbolt face plate due to overstressing of the primary support system (modified after Hoek and Marinos 2000*a*).

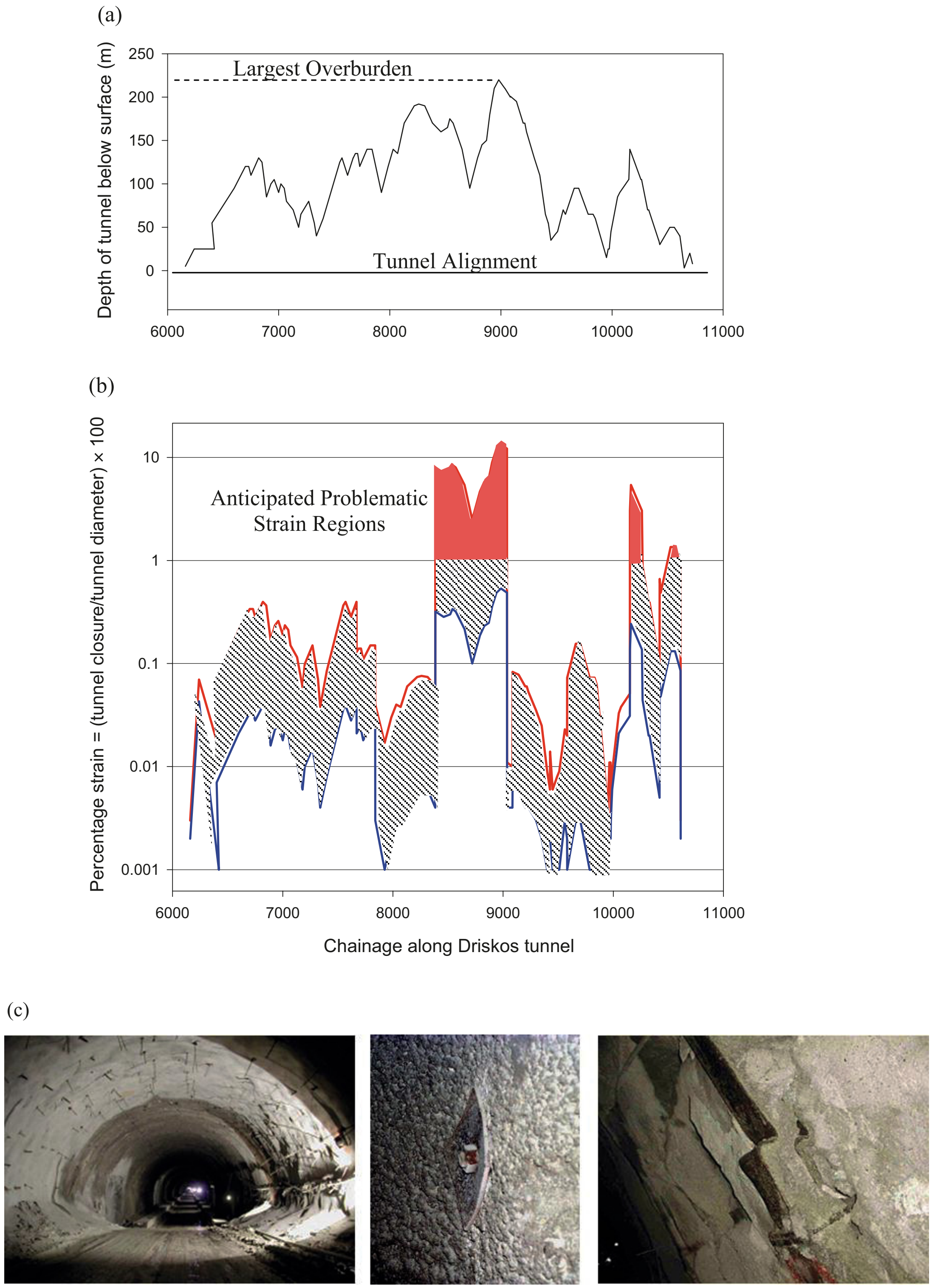

requirement (observational method) of additional support requirements due to excessive deformations. The specific characteristics, geometries, and material properties associated with these support measures are investigated in the next section.

Tunnel support measures

A longitudinal cross section of the Driskos Twin Tunnel design (category V with forepoles) is seen in Fig. 10. Here, one can see the steel-sets and the orientation of the forepole umbrella.

Fig. 7. Arrangement of tunnel support and excavation stages for horseshoe tunnel with invert, horseshoe and face support (modified after Grasso et al. 2003).

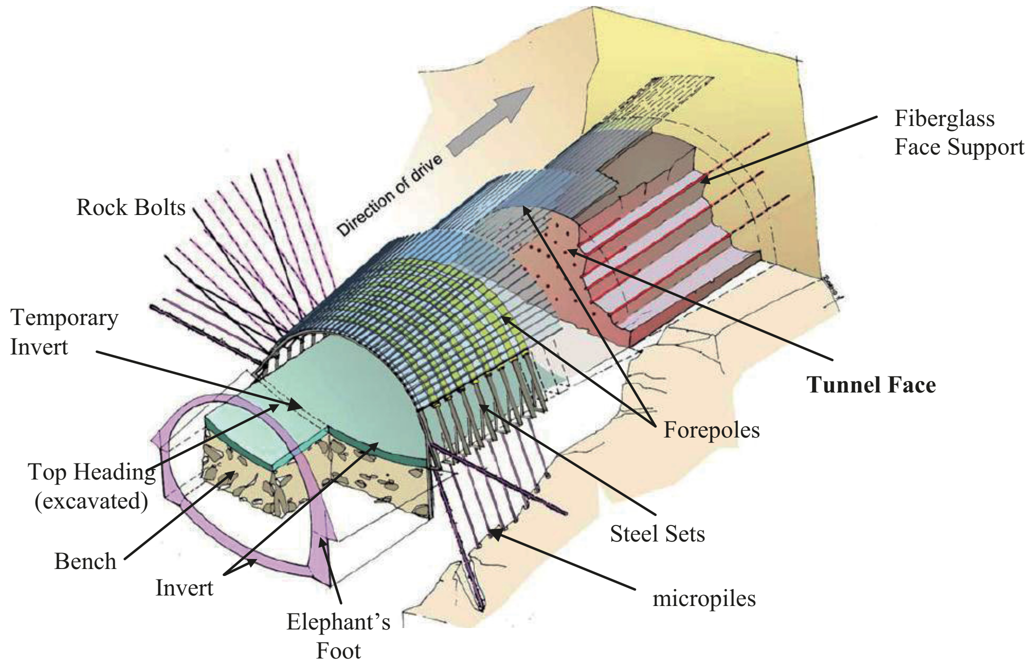

Fig. 8. (*a*) Driskos Twin Tunnel northern portals during construction in 2003 and (*b*) idealized horseshoe cross section of Driskos Twin Tunnel.

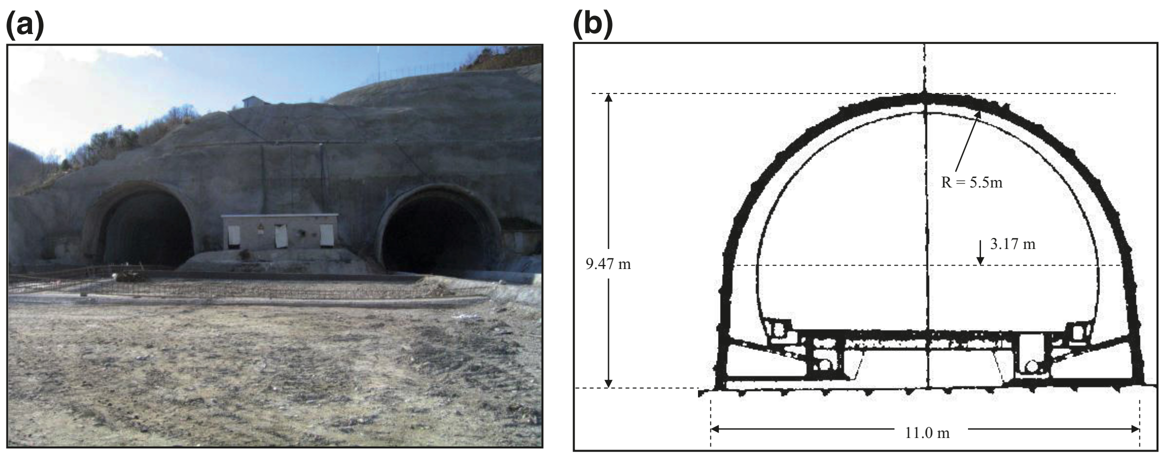

It is the weakest rock masses (and associated support category V) that were the main focus of this paper. This support category corresponds to section 4 material of the Driskos cross section (i.e., the weakest rock mass within Driskos) as cited in Fig. 5. This geological section was further divided into sub-sections to more precisely define the material according to its structure and associated strength. This is highlighted in the analysis portion of this paper.

Tunnel monitoring and behaviour

As per the observational method of tunnel design, instrumentation and monitoring play a vital role in verifying design assumptions and calibrating numerical models. As well, monitoring serves as an alert if the initial support or lining is not performing as intended or if the tunnel is in danger of collapse. Deformation is a main factor in controlling the failure and cost-effectiveness of underground excavation. As such, in the last two decades deformation monitoring has become a fundamental requirement for assessing the stability of underground openings and for quantifying the acceptable risk of rock response. (Kontogianni and Stiros 2002). Monitoring data also provides a wealth of data as to the three-dimensional (3D) behaviour of the rock mass, support, and the time history associated with excavation. This information can be used to improve geotechnical models and optimize the excavation process.

The monitoring program within the tunnels of Driskos incorporated the use of inclinometers, extensometers, strain gauges, load cells, instrumented rock bolts, and standard convergence and deformation measurements (Hindley et al. 2004). Within the concept of the observational method of tunnel construction, monitoring has also played an important role in making design changes to primary support systems. Figure 11 depicts selected monitoring instrumentation that was employed during tunnel construction for Driskos as well as other tunnels of the Egnatia Odos Highway.

The observation method includes the gathering of geodetic data in the form of surveying. This monitoring scheme was used to verify the adequacy of the adopted geomechanical model and to

Fig. 9. Original support categories II–V for Driskos Twin Tunnel (modified after Egnatia Odos, S.A. 1999).

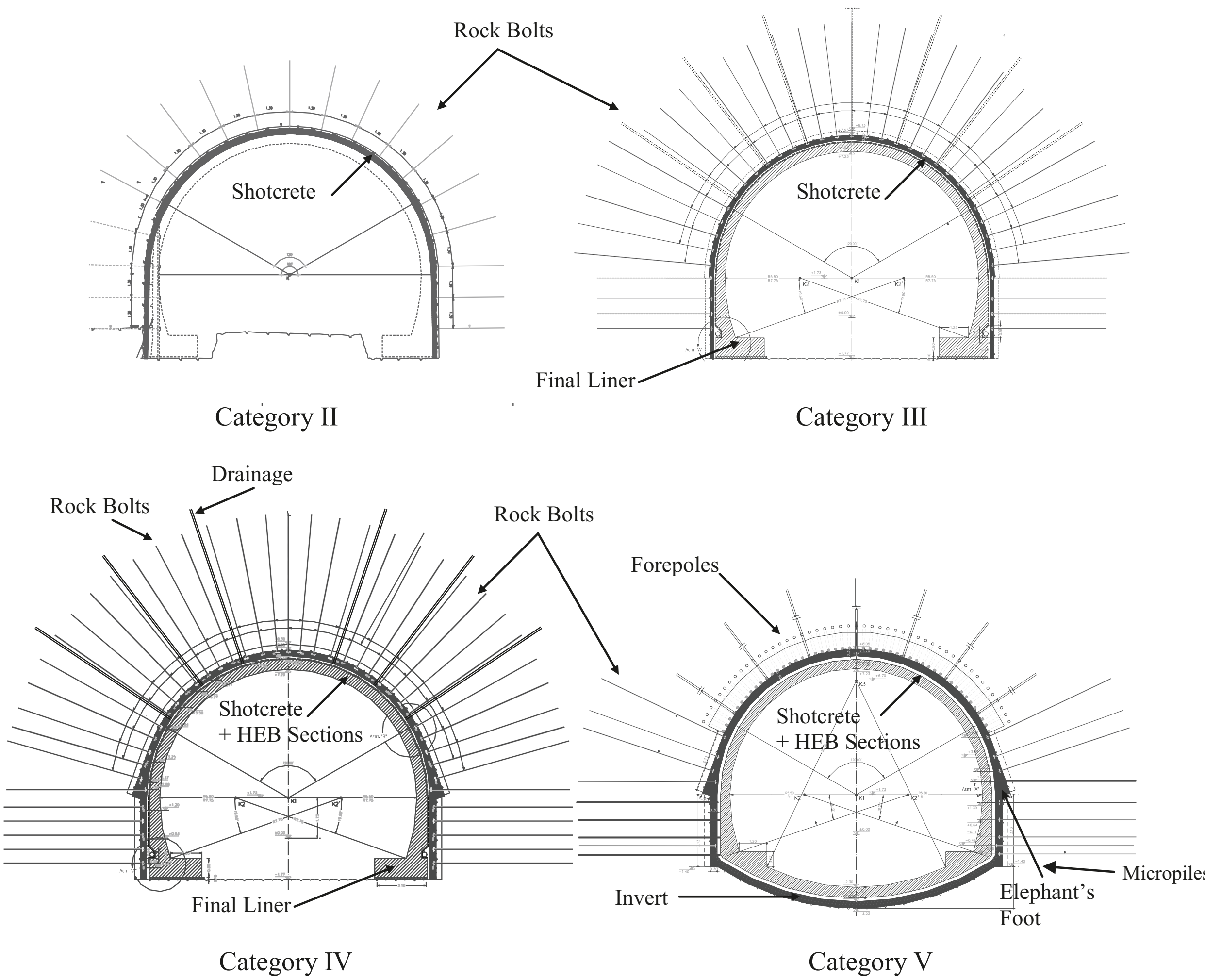

support the classification–support system. These data are paramount in making decisions on modifications to design and construction optimizations during the construction phase. A monitoring program for the tunnels of Driskos included 3D tunnel wall displacements using optical survey markers as can be seen in Fig. 12.

Figure 13 is an example of the monitoring (survey) data that was collected in the field at chainage 5 + 503 for the left bore. One can see that each survey point (from Fig. 12) was used to determine the relative closure of the tunnel excavation. Data of this nature are not only valuable in determining rock mass behaviour with a view to modifying the temporary design, they can also be used to validate numerical models and obtain rock mass parameters through back-analysis. This investigation utilized the data from the field to validate the 3D numerical model that was created to predict the behaviour of the Driskos Twin Tunnel.

Tunnelling issues associated with the Driskos Twin Tunnel construction

Prior to construction, it was predicted that section 4 of the Driskos Twin Tunnel would be the most problematic due to the weak rock masses within that section. As such, the rock mass was designated as category V and the initial design complemented this designation (Egnatia Odos, S.A. 2003). This was also predicted based on rock mass strength assumptions and in situ stresses as seen in Fig. 6.

However, the deformations that ensued due to tunnel excavation were greater than anticipated. As such, the tunnel temporary design was re-evaluated and modified after an extensive monitoring program by GeoData S.A. (Grasso et al. 2003) and design recommendations in reports by a panel of experts (Hoek and Marinos 2000*b*). Photos of the problematic section are shown in Fig. 14.

The identified problem was overstressing of the temporary–primary support that occurred at several locations during excavation and extended over distances of approximately 10 m over the tunnel alignment. This is typical of the response to be expected and is associated with large deformations due to a combination of high stress and low rock mass strength. The influence on the size of the plastic zone (Fig. 15) also plays a key mechanistic role within the expected deformation profile as examine by Vlachopoulos and Diederichs (2009). The larger the ultimate plastic zone, the larger the expected deformations as well as the interaction with the plastic zone ahead of the tunnel excavation (face).

Records of the convergence measurements showed that stable conditions were only reached 7 months after the commencement of the top heading excavation with an excess convergence that (in several locations over a 300 m segment of the alignment) exceeded 150 mm.

As well, the strength of the siltstone–sandstone flysch was reduced locally by the presence of a high concentration of parallel

Table 5. Support measures for each rock mass category for Driskos Twin Tunnel (modified after Structural Design, S.A. 1999).

Support category	Construction phases	Span of unsupported portion	Support measures: Application time	Rockbolts	Shotcrete	Steel-sets	Additional measures
II	2 (top heading–benching)	6 m	18 h from the blasting	3 m rockbolts in distribution 1.5 × 2.0 m in crown and sides	10 cm in the crown and 5 cm in the sides	—	—
III	2 (top heading–benching)	3 m	12 h from the blasting	3 m rockbolts in distribution 1.3 m × 1.3 m in crown and sides	15 cm in the crown and 10 cm in the sides	—	—
IV	4 (2 top heading–2 benching)	2 m	During excavation	4 m rockbolts in distribution 1.2 × 1.0 m in crown and sides, 6 m rockbolts in rest of crown	20 cm in the crown and the sides and 10 cm at the face of top heading	Steel-sets (HEB)	—
Va	4 (2 top heading–2 benching)	2 m	During excavation	6 m rockbolts in distribution 1.5 × 1.0 m in crown, sides and bottom	25 cm in the crown and the sides and 10 cm at face of top heading	Steel-sets (HEB)	Forepole umbrella if necessary
Vb	2 (top heading–benching)	2 m	During excavation	6 m rockbolts in the basis of the steel sets	25 cm in the crown and the sides and 10 cm at the face of the top heading; 25 cm for invert	Steel sets (HEB)	Forepole umbrella

Note: HEB, European standard wide flange H beams.

Fig. 10. Longitudinal cross section of Driskos showing tunnel support (class V) detail (modified after Structural Design, S.A. 1999).

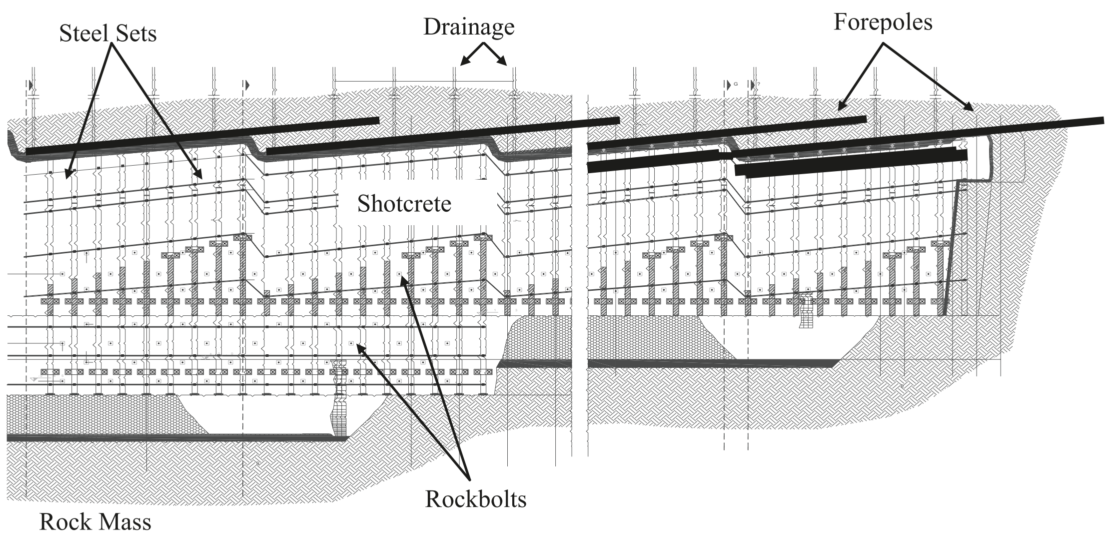

bedding crossed by frequent faults. These rock mass features within this chainage can be seen in Fig. 16. Also contributing to the excessive deformation was the presence of water that contributed to a reduction in rock mass strength.

The deformations that were observed did not exhibit a tendency to stabilize with time. The design, therefore, overestimated the rock mass strength for this particular section and as a result, the design capacity of the primary support was determined to be too low (Hoek and Marinos 2000*b*).

Another factor influencing the analysis of the rock mass is the variability of the face conditions and the anticipated behaviour of such mixed face conditions. As seen in Fig. 17, there is much variability of the face conditions within a limited change distance. Within 60 m (or ~5.5 × tunnel diameter), the sandstone and siltstone layers go from having a horizontal layering arrangement to a vertical orientation. At a larger scale, however, as presented in Fig. 4, the general trends of the larger weak masses are clearly evident. In this way, anisotropy at the tunnel scale is not anticipated. Figure 18 also captures the variability of the ground conditions at depth within a limited scale. The results from the numerical modelling (as described in the following sections) indicate that a “homogenization” of the face at these depths and at these scales is suitable to capture the overall behaviour of the tunnel.

A rigorous monitoring program was implemented to capture deformations and modify the support categories. As a summary, the major observations associated with the monitoring program as well as their implications for the re-design of the temporary support for section 4 of the Driskos Twin Tunnel were (Egnatia Odos, S.A. 2001):

1. During the top heading phase of excavation, 210 mm of tunnel closure was exhibited by the primary–temporary support.
2. Upon excavation of the parallel bore, 310 mm of displacement was captured.

Fig. 11. Instrumentation and targets associated with monitoring program of the Egnatia Odos Highway: (*a*) monitoring well and survey target on benchmark, (*b*) pressure cell (left) and extensometer (right), (*c*) tunnel wall pressure cell, (*d*) tunnel wall survey target, (*e*) surveying the tunnel face, and (*f*) measurement of targets on tunnel wall (–19 denotes 19 mm of inward displacement at that target location) within Driskos Twin Tunnel.

Fig. 12. Optical survey markers and their locations within the tunnel excavation. Note that A-Phase and B-Phase are analogous to top heading and bench excavation phases, respectively.

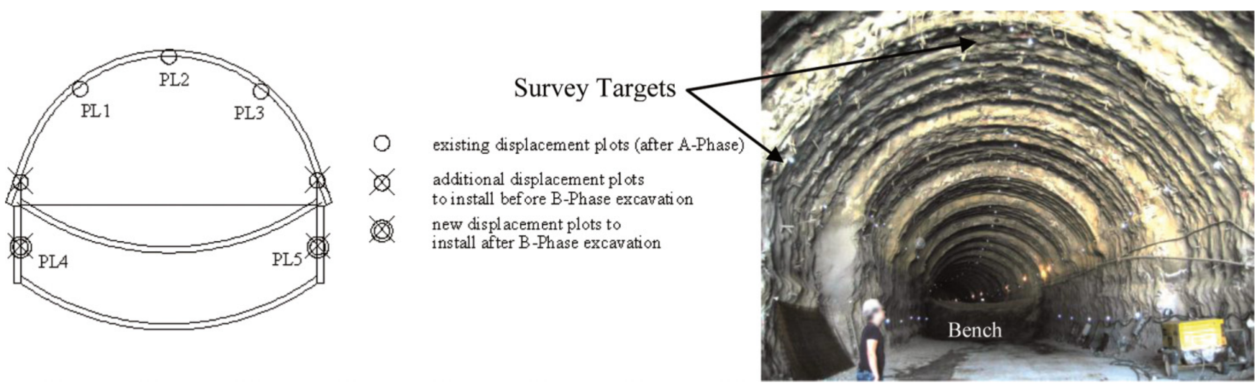

3. Additional primary support measures included closer spacing of steel-set support sections, more and longer fully grouted rockbolts, thicker shotcrete shell, introduction of prestressed cable anchors, and the introduction of an invert.
4. Micropiles were also included into the re-design of the temporary support. They were incorporated as a steel-reinforced continuous concreted beam element that was laid at the base of the steel ribs along each sidewall.

Deformations were on average larger on the outer sidewalls indicating asymmetric tunnel closure behaviour. This was not predicted at the initial design phase for the primary support. More symmetric conditions were achieved after the modification of the sidewall rockbolt pattern was implemented. Another factor that influences this behaviour is a realistic evaluation of the stress field conditions.

Methods of analysis

Convergence–confinement and longitudinal displacement profile (LDP)

Convergence–confinement analysis (Duncan-Fama 1993; Panet 1993, 1995; Carranza-Torres and Fairhurst 2000; as well as others) is a commonly accepted tool for preliminary assessment of squeezing potential and support requirements for circular tunnels in a variety of geological conditions and stress states. It is within this convergence–confinement framework that tunnel behaviour was analyzed within this paper, with particular emphasis on the longitudinal displacement profile (LDP) portion of this concept.

To determine the appropriate timing for the installation of preliminary support systems or when optimizing the installation of support with a view of specific displacement capacity, it is important to determine the longitudinal closure or displacement profile for the tunnel. A portion of the maximum radial displacements at the tunnel boundary will take place prior to the advancement of the face past a specific point. The tunnel boundary will continue to displace inwards as the tunnel advances further beyond the point in question. This longitudinal profile of closure or displacement versus distance from the tunnel face is called the longitudinal displacement profile or LDP.

Panet and Guenot (1982), Panet (1993, 1995), Chern et al. (1998), and others have proposed empirical solutions for LDPs based on

Fig. 13. Radial convergence as captured by survey data from Driskos left bore at chainage 8 + 503.

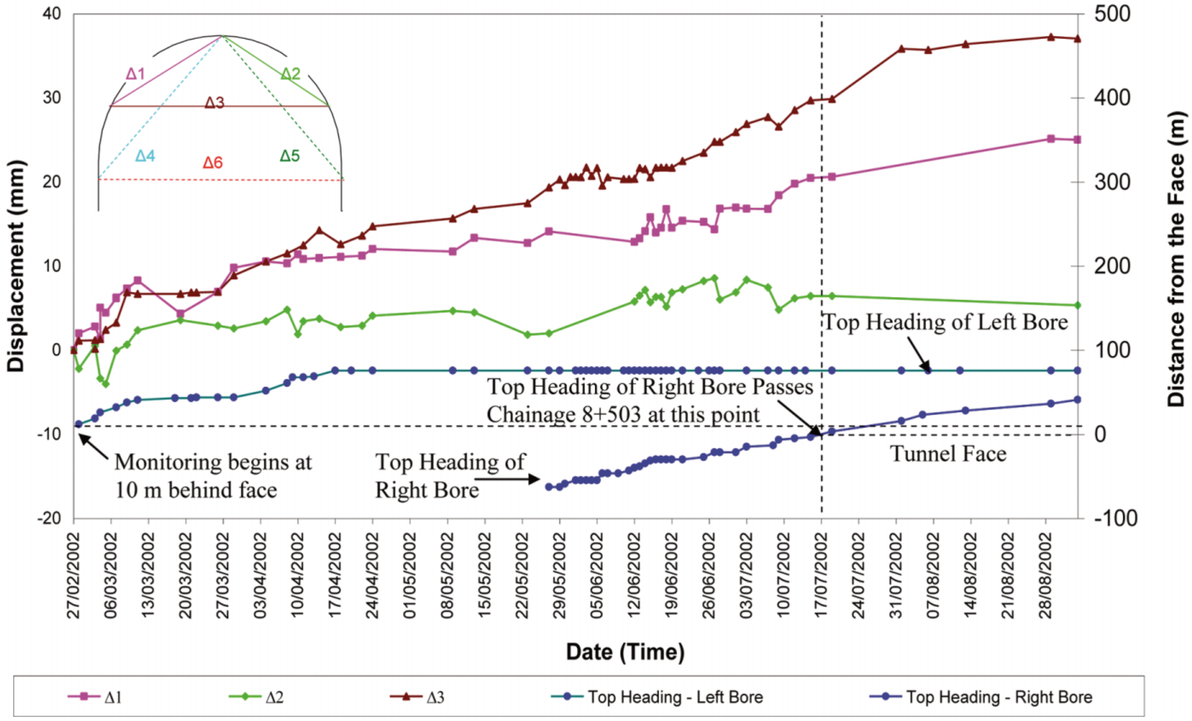

Fig. 14. Excessive deformations experienced within section 4 of Driskos Twin Tunnel: (*a*) deformed rockbolt face plate as a result of overstressing of the primary support; (*b*) spalling of the shotcrete adjacent to a stressed steel set, (*c*) sidewall of Driskos Twin Tunnel denoting (in red in Web version of this paper and medium grey in print version) the total amount of inward displacements at selected, monitored target points; and (*d*) clearer designation of inward displacement in millimetres.

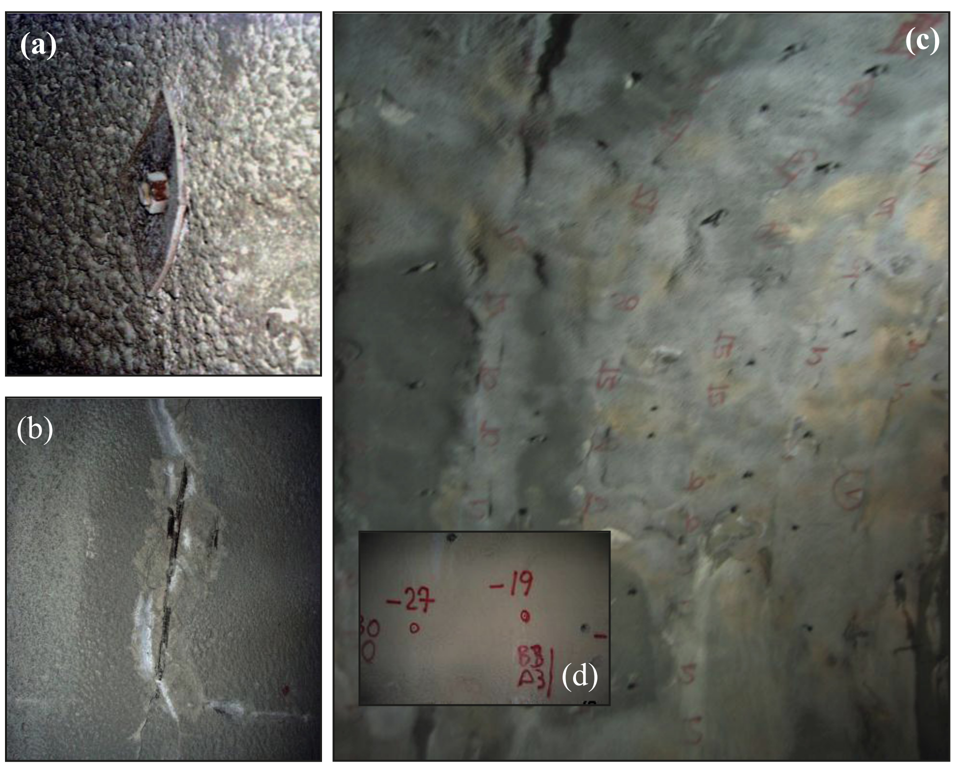

elastic modelled deformation of varying intensity (correlated to various indices such as the ratio between in situ stress and undrained cohesive strength, for example). Alternatively, an empirical best fit to actual measured closure data can be used (i.e., based on data from Chern et al. 1998). These solutions have been well documented in Vlachopoulos and Diederichs (2009).

The case study presented herein highlights the requirement for a better assessment of rock mass strengths and field values as well

Fig. 15. Plastic yield zone (*bullet-shaped, shaded zone*) developing as tunnel advances to the left from axisymmetric finite element method (FEM) analysis. If (*a*) the wall yield zone is more than double the tunnel radius (*R*) it interacts with the face yield zone; however, (*b*) if the maximum plastic zone radius is less than twice the tunnel radius, the wall yield zone does not interact with the face yield zone.

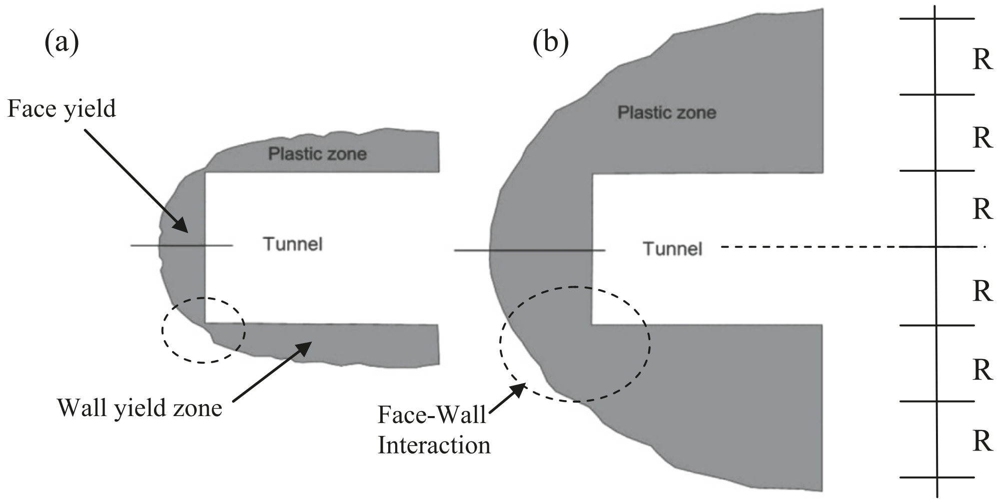

Fig. 16. Photo and sketch of tunnel face in flysch within problematic region (modified after Egnatia Odos, S.A. 1999).

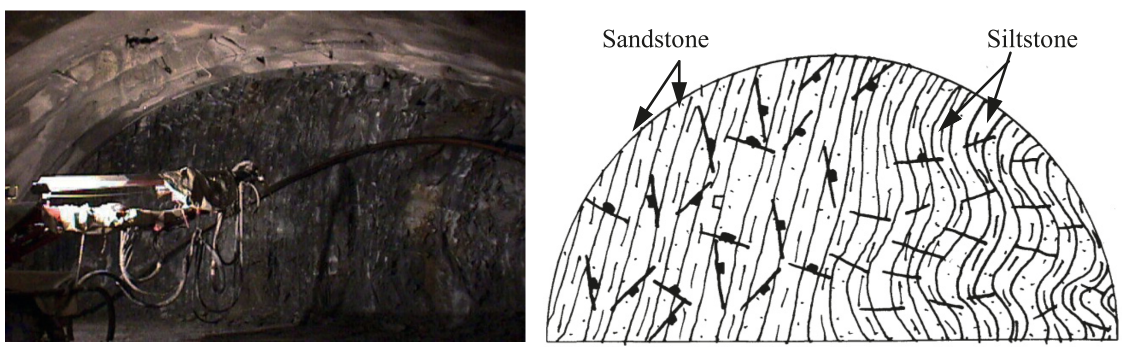

Fig. 17. Sketches of tunnel faces in flysch during excavation of Driskos Twin Tunnel (modified after Egnatia Odos, S.A. 1999).

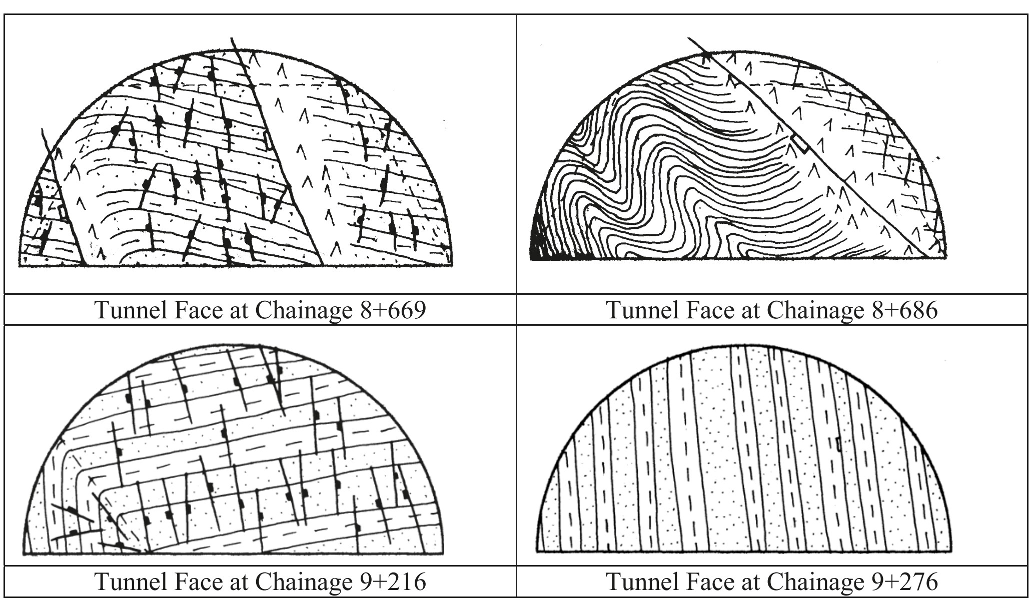

Fig. 18. Results of intense tectonism in rock masses within the region.

as more accurate predictive tools in terms of rock mass behaviour associated with tunnel excavation. As such, the accurate monitoring data that were amassed as part of the Driskos Twin Tunnel construction were used in this investigation to validate the 3D and 2D numerical models that were specifically created for this research study. The data was also used for back-analysis purposes.

The themes of this investigation relate to how well the Driskos monitoring data correlate to the theoretical empirical formulations, how the selection of GSI affects tunnel design, which LDP does a designer use to determine the appropriate tunnel support (i.e., unsupported or supported LDP), the effectiveness of the support, and what the effect is of twin tunnel interaction among other considerations.

Numerical models

Within this investigation, Phase2 (Rocscience Inc. 2004–2007) was used for the 2D numerical analysis and FLAC3D (Itasca 2002–2005) was used for the 3D numerical analysis. Phase2 uses an implicit finite element method (FEM) while FLAC3D employs the finite difference method (FDM) in its determinations. Both of these programs are widely used in the geotechnical and geological engineering industry to capture the behaviour of a tunnel (i.e., stress re-distributions and displacements) associated with tunnel excavation. Cai (2008) also investigated the numerical modelling codes for Phase2 and FLAC (2D) (the basis of FLAC3D) on the influence of stress path on tunnel excavation response and these findings will not be repeated here. Cai stated that one software package was not superior to the other, rather he points out the importance of understanding the program codes and selecting the right tool and modelling approach to represent the expected stress path as close to reality as possible. The emphasis in comparison therefore, should not lie in the limitations of the software packages, but on the details of how the true physical phenomenon is being modelled within these limitations. These modelling considerations have been investigated for deep, high-stress circular and horseshoe tunnels in weak rock masses by Vlachopoulos and Diederichs (2009).

Three-dimensional (3D) analysis

FLAC3D (Itasca 2002–2005) is an explicit finite difference program that is used to study the mechanical behaviour of a continuous 3D medium as it reaches equilibrium or steady plastic flow. Selected geometries associated with the 3D model that was developed for the purposes of this investigation can be seen in Fig. 19. This model consists of the horseshoe twin tunnel configuration that is associated with the Driskos Twin Tunnel. The model includes similar excavation geometries incorporating sequential excavation and support. The numerical model that was created uses FLAC3D group zones. The model is 110 m in height and 110 m wide with a tunnel length of 80 m. To reduce boundary effects, the tunnel excavation occurred at the centre of the block surrounded further by a series of abutments. The excavated material within the tunnel was created separately and was subdivided into subsections that constituted an excavation step and could be separated into full-face or top heading–bench excavation. At each unsupported excavation step, an excavation sub-section block was nullified and steps were conducted to ensure equilibrium conditions were met prior to the next excavation sequence. In terms of support, a forepole support umbrella (pile element) was installed and allowed to reach equilibrium prior to each excavation step as per the support installation and excavation steps conducted in the field. The tunnel lining consisted of a 30 cm thick shotcrete layer that was replicated using liner elements. Support detail is seen in Fig. 20.

Two-dimensional (2D) analysis

Phase2 is a 2D, implicit, elastoplastic FEM program used to calculate stresses and determine displacements around underground tunnels and can be used to solve a broad range of geotechnical problems. Phase2 uses plane strain analysis whereby two principal in situ

Fig. 19. Selected geometries associated with 3D (FLAC3D) and 2D (Phase2) numerical models used in this investigation. Also, inset is an idealized cross section of a Driskos Twin Tunnel bore.

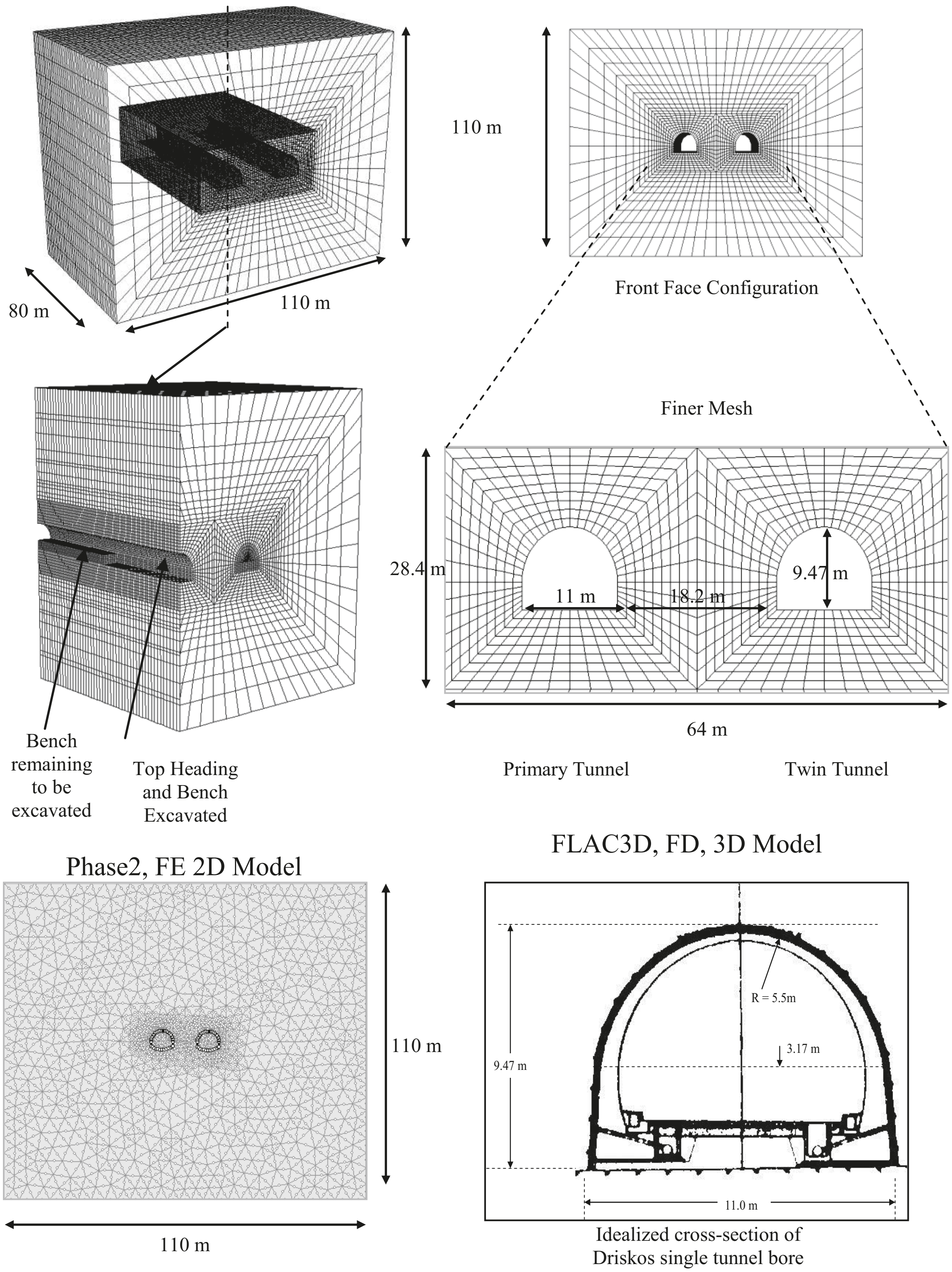

stresses are in the plane of the excavation and the third principal stress is out of plane. As with other finite element regimes, the domain is discretized into a set number of elements and corresponding nodes. Displacements within these finite elements are calculated based on shape functions tied to the nodes of the elements (Rocscience Inc. 2004–2007). Initial in situ stresses, tolerance parameters, and material and defect properties are all assigned by the user. Tunnel excavation is simulated by the removal of elements from within an excavation boundary located in an external boundary.

A selected geometry of one of the 2D numerical models that were developed for the purposes of this investigation can be seen within Fig. 19. Again, the Driskos Twin Tunnel case study horseshoe geom-

Fig. 20. Support detail within the twin tunnel FLAC3D numerical model (only excavated material and support components are shown).

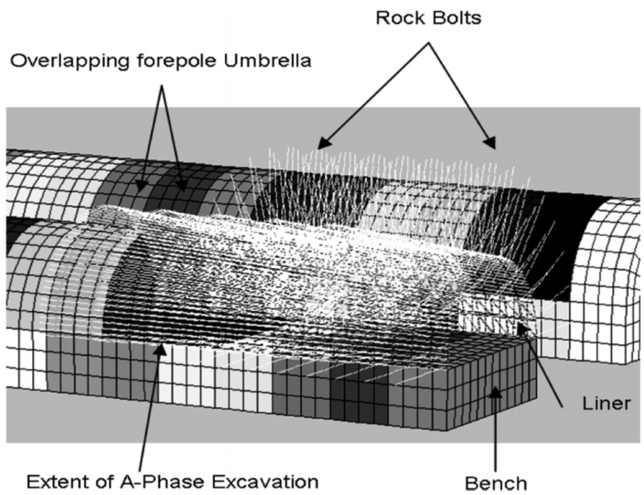

etry was replicated for the 2D model. These models mimicked a cross-sectional plane of the 3D models described in the previous section.

Analysis details

The runs that were conducted consisted of supported and unsupported simulations with elastic – perfectly plastic models (Mohr–Coulomb constitutive model within FLAC3D), strain-softening (residual strength), and elastic models to isolate the elastic behaviour. The problematic section within Fig. 5 was section 4.

Within this section, it was found that there were many geological differentiations that warranted further subsections to be classified and assessed. The subsections (4.1, 4.2, 4.3, 4.4, and 4.5) created for this investigation can be seen in Fig. 21. The materials and input parameters were selected to correspond to these five subsections of the geological section 4 of the Driskos alignment.

The parameters or properties associated with each of these materials are located in Table 6. These GSI and strength values were determined independently by the authors. Mohr–Coulomb equivalent properties were obtained using the Hoek–Brown failure criterion (Hoek et al. 2002). Plots of Hoek–Brown and Mohr–Coulomb criteria for these materials are seen in Fig. 22. This figure contains Hoek–Brown plots of (*a*) major and minor principal stresses, (*b*) shear and normal stresses, as well as Mohr–Coulomb plots of (*c*) major and minor principal stresses and (*d*) shear and normal stresses. Table 7 summarizes the key numerical modelling runs that were conducted for this investigation. Selected results of the major observations are presented in the next section.

Results of analysis

Geological strength index (GSI)

There is an inherent difficulty of assigning reliable numerical values to rock masses; however, the application of GSI has proven advantages when dealing with weak rock masses such as those found at Driskos. The assignment of a GSI value to a rock mass based on a qualitative assessment of rock mass structure and surface quality is a nontrivial exercise. When assigning a GSI value to a rock mass the most acceptable practice is to assign a range of GSI rather than a single value. The assessment of the strength of the rock mass will have direct implications to the design of the support to be used in a particular excavation.

In the axisymmetric, 2D finite element (Phase2) simulation that was conducted (as shown in Fig. 23), one can clearly see the effects of varying the GSI of a rock mass. On one side of the tunnel, a GSI of 35 was used, while on the other side a GSI of 45 was assigned.

A larger plastic zone of 3 diameters was associated with the lower GSI value than with the 2 diameter plastic zone that was created by the higher GSI designation. This has implications to the expected tunnel displacements and ultimately to the design of the temporary support for the excavation. The effect of the size of the plastic zone is the topic of the next section.

Hoek and Marinos (2000*a*) introduced the concept of the determination of support requirements for circular tunnels within a hydrostatic stress field through the use of dimensionless plots of the ratio of tunnel deformation to tunnel radius against the ratio of rock mass strength (as determined through the use of GSI) to the in situ lithostatic stress. From the results of numerous tunnels excavated in weak rock, the pattern that emerged followed the following empirical formulation:

$$[2] \qquad \frac{\Delta R}{R_0} = \left(0.002 = 0.0025\frac{p_i}{p_o}\right)\frac{\sigma_{cm}}{p_o}^{[2.4(p_i/p_o)-2]}$$

where
ΔR = change in tunnel radius
R_0 = original tunnel radius
p_i = internal support pressure
p_o = in situ stress = depth below surface × unit weight of rock mass
σ_{cm} = compressive strength of the rock mass (as determined by GSI).

It was also observed that once the rock mass strength falls below 20% of the in situ stress level, deformations increased substantially. Unless these deformations are controlled through the installation of adequate support mechanisms, collapse of the tunnel is likely to occur. In this manner, these plots give an excellent indication of the influence of support pressures on tunnel deformation.

The determination of σ_{cm} has always been a challenge to designers. It also proved to be a challenge for this research undertaking. An index value for uniaxial rock mass strength is given below by Hoek (1999) and Hoek and Marinos (2000*a*), respectively,

$$[3] \qquad \sigma_{cm} = 0.019\sigma_{ci}e^{0.05\mathrm{GSI}}$$

$$[4] \qquad \sigma_{cm} = \left(0.0034m_i^{0.8}\right)\sigma_{ci}\left(1.029 + 0.025e^{-0.2m_i}\right)^{\mathrm{GSI}}$$

As well, the value of strain (ε) as a function of stress (σ_{cm}) provided by Hoek and Marinos (2000*a*) is shown below

$$[5] \qquad \varepsilon = 100\left(0.02 - 0.025\frac{p_i}{p_o}\right)\frac{\sigma_{cm}}{p_o}^{[2.4(p_i/p_o)-2]}$$

For this investigation, the three methods shown in Fig. 24 were used to assess the rock mass strength of the five subsections of materials (4.1–4.5) utilized in this study. It can be seen that the original version correlated to the expected results of the data strength values the best. The Hoek (1999) version was based on a simple relationship using σ_{ci} and GSI. The Hoek and Marinos (2000*a*) version was an attempt (without real data verification) to incorporate the effect of different frictional properties (m_i) into the strength determination. The strength determination from such an equation may be too sensitive for low *m* values as it tries to capture the range of *m* from 7 to 35. Lastly, Hoek et al. (2002) is an approximation of the unconfined compressive strength (UCS) given by the cohesion and friction which are a function of confinement that were chosen to fit. In this way, it is implied that UCS is a function of confinement, which may not be entirely the case.

Using this relationship (Hoek 1999), Fig. 25 is a graph of tunnel deformation to tunnel radius against the ratio of rock mass strength (GSI) to the in situ stress for sub-sections 4.1–4.5 in terms of the total displacements observed during the excavation of a

Fig. 21. Subsections of geological section 4 of Driskos, referencing Fig. 5.

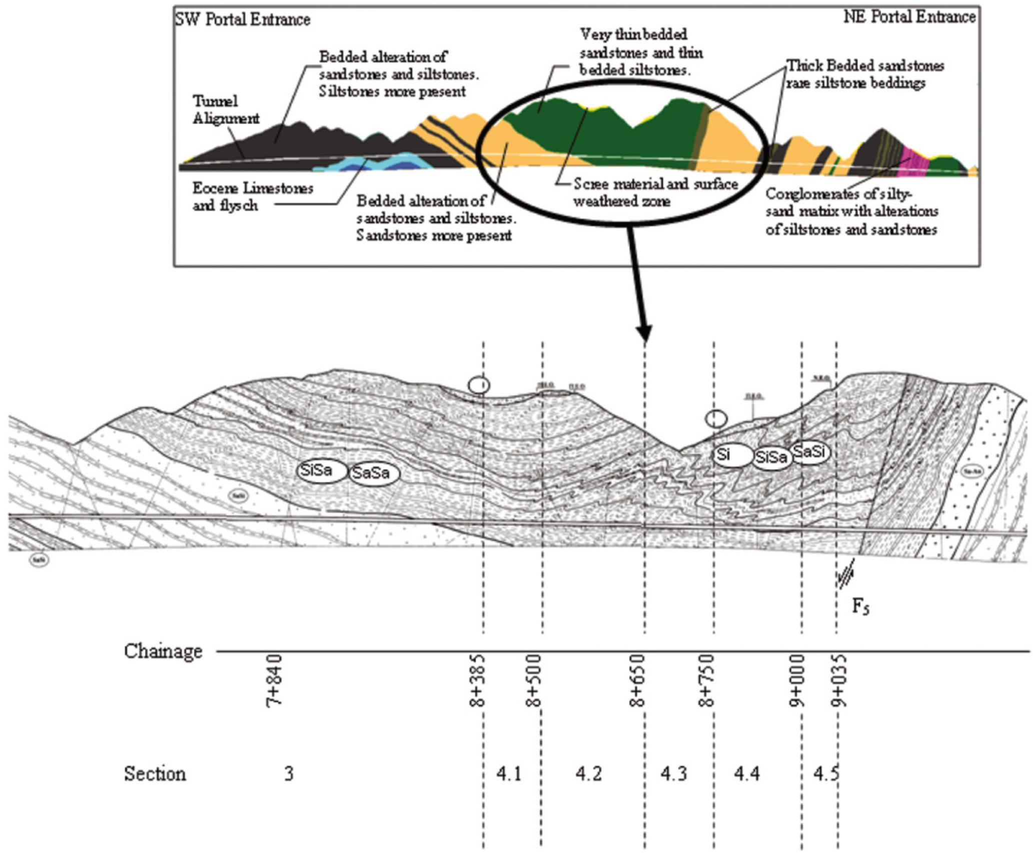

Table 6. Relevant factors and rock mass properties for subsections of geological section 4 of Driskos.

Parameter	Section 4.1	Section 4.2	Section 4.3	Section 4.4	Section 4.5
Chainage	8+385–8+500	8+500–8+650	8+650–8+750	8+750–9+000	9+000–9+035
Flysch category	B-C	B-C	E-F	E-F	B
Lithology	SiSa	SiSa	SiSa, Si	Si, SiSa	SaSi
Rock mass category	IV–V	IV	III– IV	III–IV	III– IV
Overburden (m)	145	130	100	180	220
ν	0.25	0.25	0.25	0.25	0.25
Hoek–Brown					
GSI	18–41	21–30	22–40	31–40	35–41
GSI avg	29.5	25.5	31	35.5	38
σ_{ci} (MPa)	37.5	37.5	26.25	26.25	75
m_i	10.3	10.3	7.75	7.75	17
E_i (MPa)	16125	16125	13453.1	13453.1	28125
D	0	0	0	0	0
m_b	0.83	0.72	0.66	0.77	1.8
s	0.000396	0.000254	0.000468	0.000772	0.001019
a	0.52	0.53	0.52	0.52	0.51
Mohr–Coulomb					
c (MPa)	0.44	0.37	0.29	0.46	1.02
ϕ (°)	38	37	36	33	47
σ_t (MPa)	−0.017	−0.013	−0.018	−0.026	−0.041
σ_c (MPa)	0.62	0.46	0.48	0.65	2.18
σ_{cm} (MPa)[a]	3.1	2.5	2.3	2.9	9.5
E_{rm} (MPa)[b]	1576.2	1244.1	1442.1	1901.0	4127.7
σ_{cm}/p_o	0.84	0.77	0.92	0.64	1.70

Note: ν, Poisson's ratio; E_i, intact rock modulus of elasticity; D, degree of disturbance factor; c, cohesion; σ_{cm}, compressive strength of the rock mass (as determined by GSI).

[a]Simplified (original) formula from Hoek (1999).

[b]Average value of Hoek et al. (2002) and Hoek and Diederichs (2006).

Fig. 22. Comparison of Hoek–Brown and Mohr–Coulomb strength parameters for subsections 4.1–4.5. Hoek–Brown plots of (*a*) major and minor principal stresses and (*b*) shear and normal stresses; Mohr–Coulomb plots of (*c*) major and minor principal stresses and (*d*) shear and normal stresses.

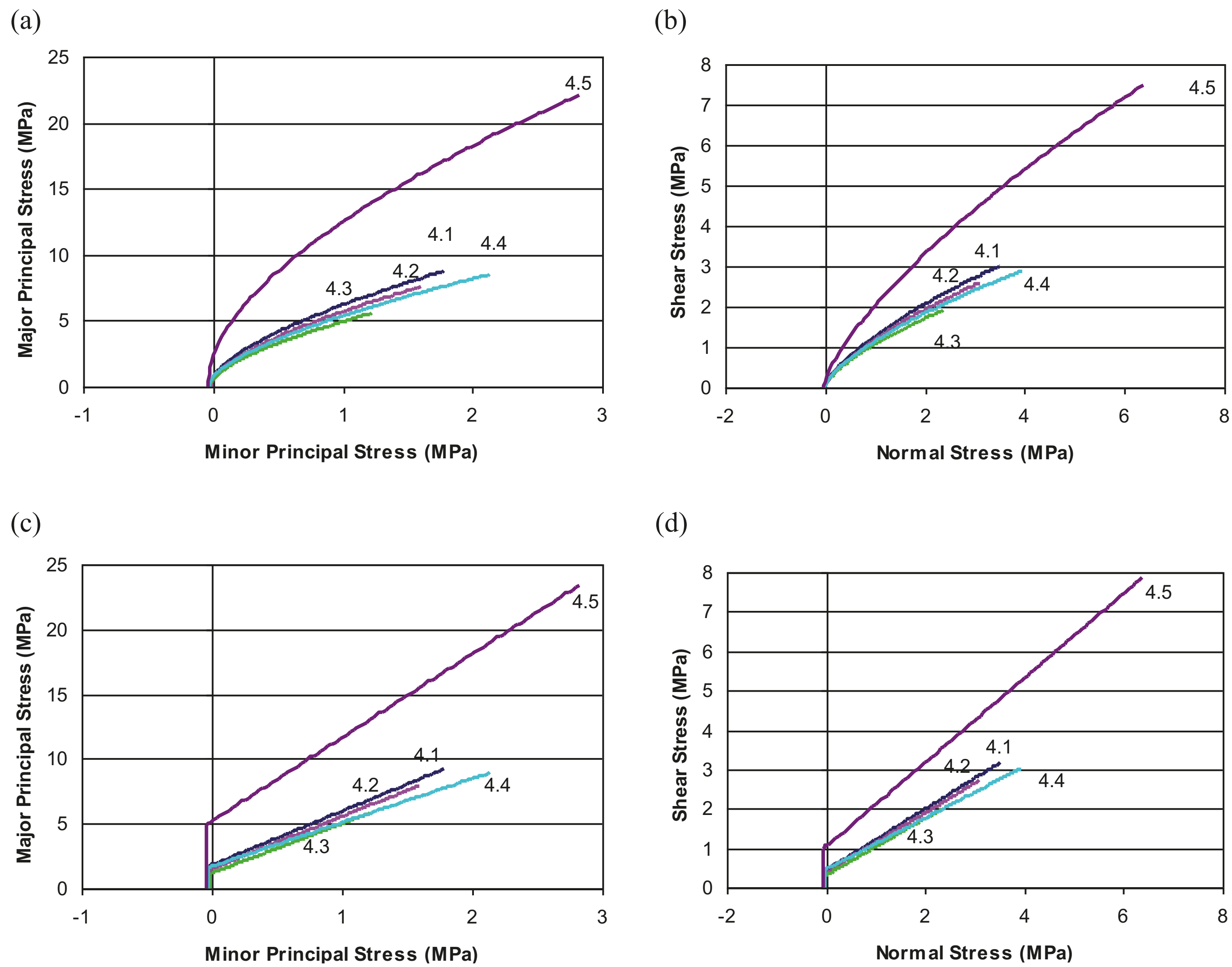

Table 7. Selected numerical modeling runs used in this investigation.

Materials	Constitutive model	Support	Dilation angle (°)	Notes
4.1–4.5	Elastic, perfectly plastic	Unsupported	0	—
4.1–4.5	Elastic, perfectly plastic	Supported	0	—
4.1–4.5	Strain-softening (brittle)	Unsupported	0	Residual strength = 80%
4.1–4.5	Strain-softening (brittle)	Supported	0	Residual strength = 80%
4.1–4.5	Strain-softening (brittle)	Unsupported	Peak 10; Residual 0	Residual strength = 80%
4.1–4.5	Strain-softening (brittle)	Supported	Peak 10; Residual 0	Residual strength = 80%
4.1–4.5	Perfectly elastic	Unsupported	0	—
4.2, 4.4	Elastic, perfectly plastic	Supported top heading and invert	0	Install liner at face
4.2, 4.4	Strain-softening (brittle)	Supported top heading and invert	0	Install liner at face
4.2, 4.4	Strain-softening (brittle)	Supported top heading and invert	Peak 10; Residual 0	Install liner at face
4.2, 4.4	Elastic, perfectly plastic	Supported top heading and invert	0	Install liner 8 m from face
4.2, 4.4	Strain-softening (brittle)	Supported top heading and invert	0	Install liner 8 m from face
4.2, 4.4	Strain-softening (brittle)	Supported top; heading and invert	Peak 10; Residual 0	Install liner 8 m from face

single tunnel without the influence of the twin tunnel. Superimposed on the graph are the monitoring values from the field, supported and unsupported values as obtained from the 3D FLAC3D numerical analysis as well as plots of varying support pressures (p_i/p_o).

Figure 26 is a plot similar to Fig. 25; however, this plot takes into consideration the influence of the twin tunnel. One can clearly observe the worst rock mass section (in terms of empirically derived and modelling results) is that of subsection 4.4. A GSI strength assessment will directly affect the alignment of the rock mass value on the strength axis (*x*-axis), having a direct impact on support decisions. The rock mass strength for section 4.4 (and all other sections) does not fall below 20% of the in situ stress level, thus not requiring an extreme temporary support system to be

Fig. 23. Yield-related closure (no gravity) of two unsupported tunnels at 300 m depth using axisymmetric FEM analysis (grid distortion × 10).

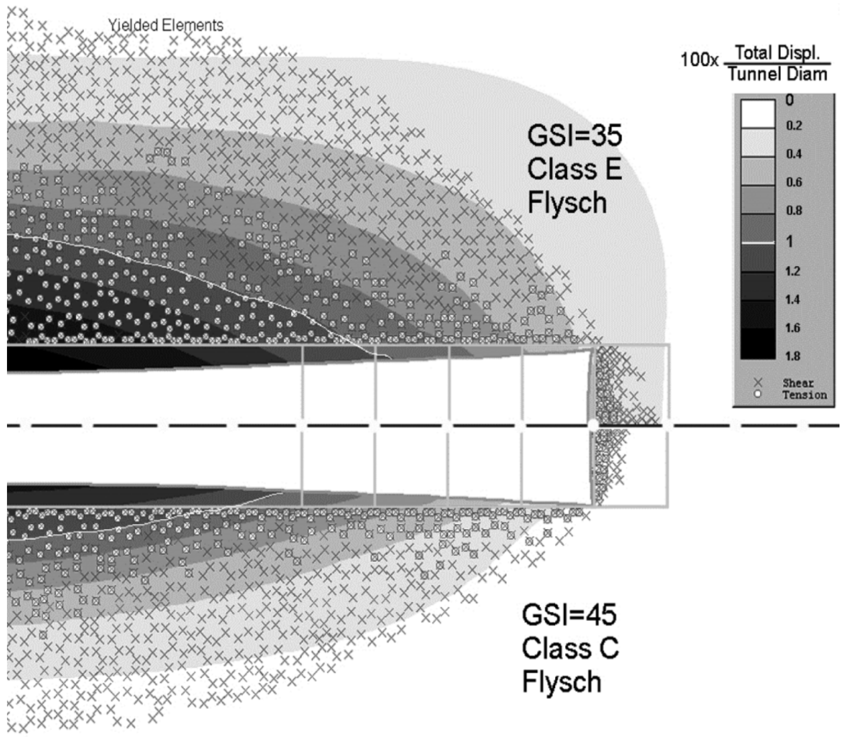

Fig. 24. Comparison of model data with normalized tunnel closure predicted by Hoek and Marinos 2000*b* (p_i/p_o = normalized support pressure). Rock mass strength is calculated according to three evolutions of this index according to the references shown. The original 1999 version correlates with the modelling data.

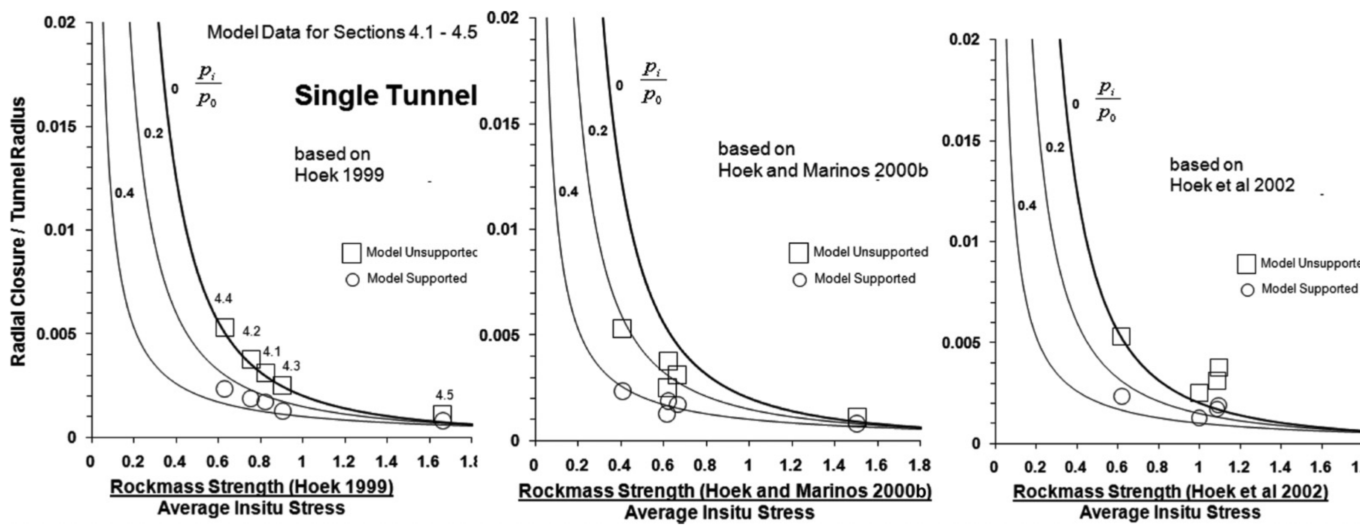

implemented. Figure 25 demonstrates that the upper and lower bounds of the monitoring data that were observed in the field were accurately captured by the numerical modelling simulations. There are some outliers (boxed by a dotted square in this figure) that further reinforce the notion that over the entire length of the tunnel, it is impossible to characterize fully all of the conditions that will be encountered. Localized and unidentified (and thus unclassifiable) fault zones as well as other geological peculiarities can add to the degradation of the strength of the rock mass in certain regions. These occurrences can be seen for subsections 4.2 and 4.3. In terms of the Driskos Twin Tunnel construction, when such observances occurred, tunnelling experts were consulted to provide advice, modify the design, and offer quality control with a view to managing the situation and reducing or eliminating such incidents.

Longitudinal displacement profile (LDP)

As mentioned previously, the LDP is one of the basic components of the convergence–confinement method. It is a graphical representation of the radial displacement that occurs along the axis of an unsupported cylindrical excavation prior to and past the face. Figure 27 depicts such a profile. The horizontal axis indicates the distance from the face and the vertical axis indicates the corresponding tunnel wall displacement. At a certain distance ahead of the face, the advancing tunnel has no influence on the rock mass and the radial displacement is zero. At approximately 1

Fig. 25. Ratio of tunnel deformation to tunnel radius versus the ratio of rock mass strength to in situ stress for varying support pressures with Driskos monitoring data as well as unsupported and supported 3D modelling analysis for single tunnel.

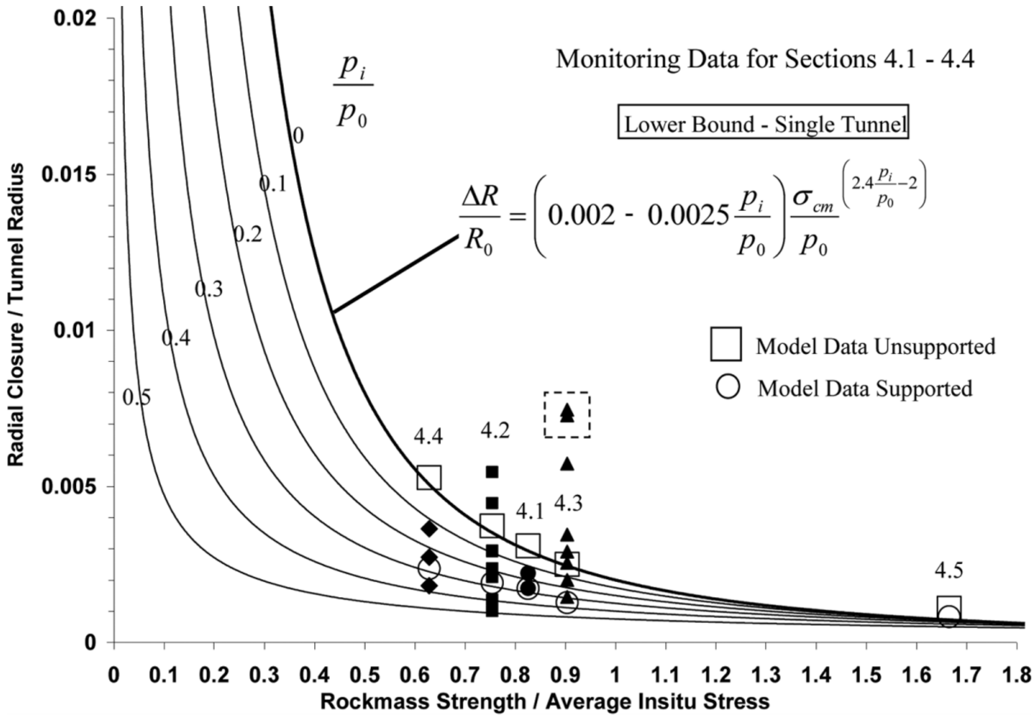

Fig. 26. Ratio of tunnel deformation to tunnel radius versus the ratio of rock mass strength to in situ stress for varying support pressures with Driskos monitoring data as well as unsupported and supported 3D modelling analysis for single tunnel taking into account the displacements due to parallel (twin) bore excavation.

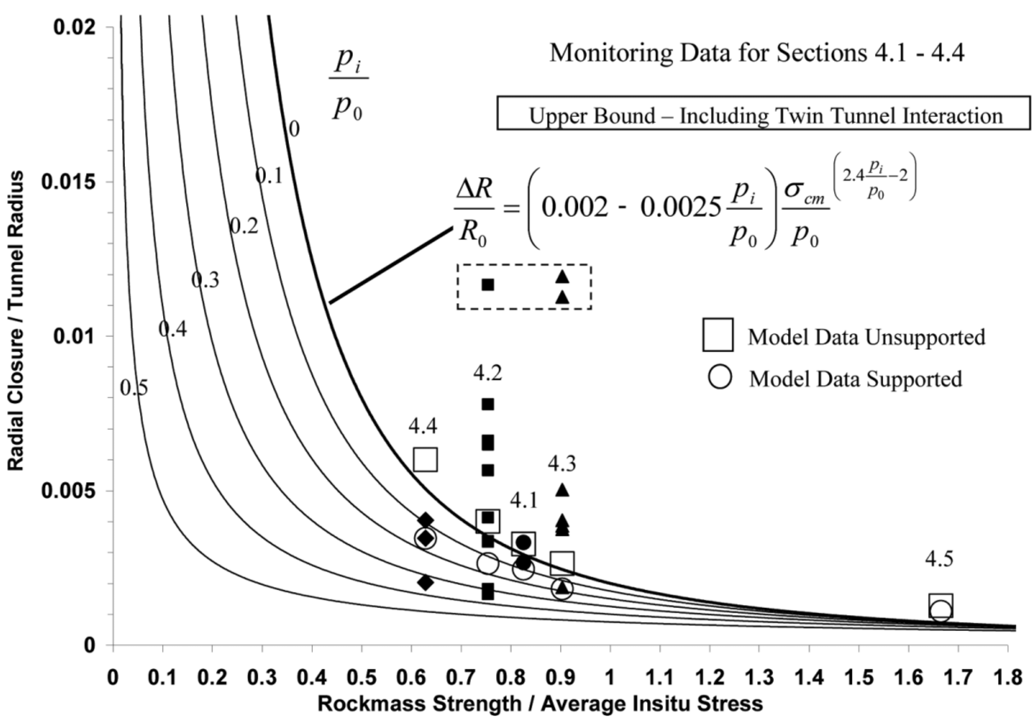

diameter distance ahead of the face, the rock mass begins to influence the rock mass. At the face, approximately 30% of the total displacement has already occurred and at a certain distance past the face, the effect of the face is substantially reduced as displacements stabilize.

The LDPs associated with Panet (1995) and Unlu and Gercek (2003) are plotted in Fig. 28. Also plotted in this figure are the LDPs associated with 12 monitored sections within the Driskos Twin Tunnel. Note that all of the data has been normalized with respect to the maximum supported displacement and the original radius

Fig. 27. Typical longitudinal displacement profile for an advancing tunnel within a weak rock mass.

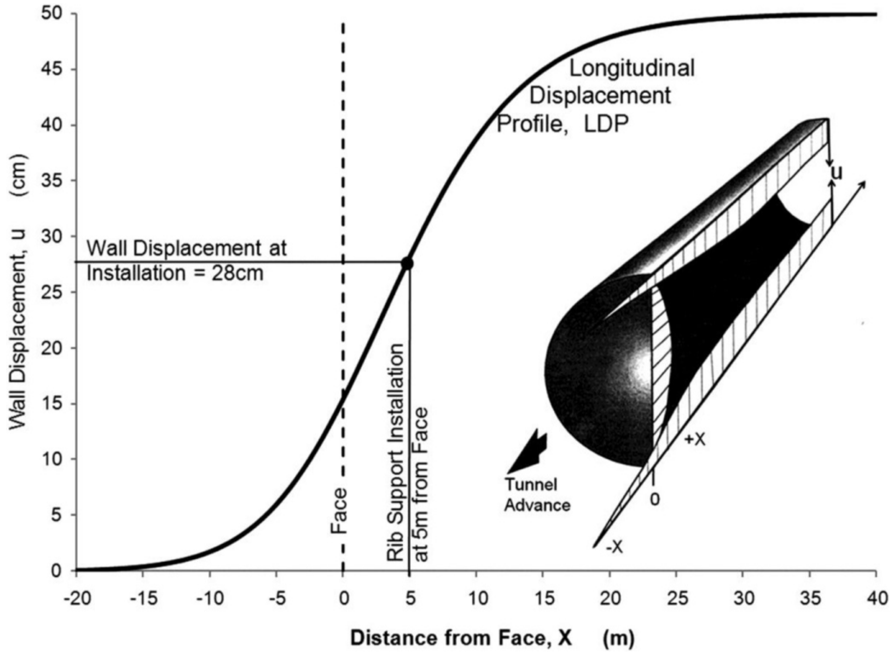

Fig. 28. Longitudinal displacement profiles associated with the empirical formulations of Panet (1993) and Unlu and Gercek (2003) as well as the LDPs of monitored sections of the Driskos Twin Tunnel.

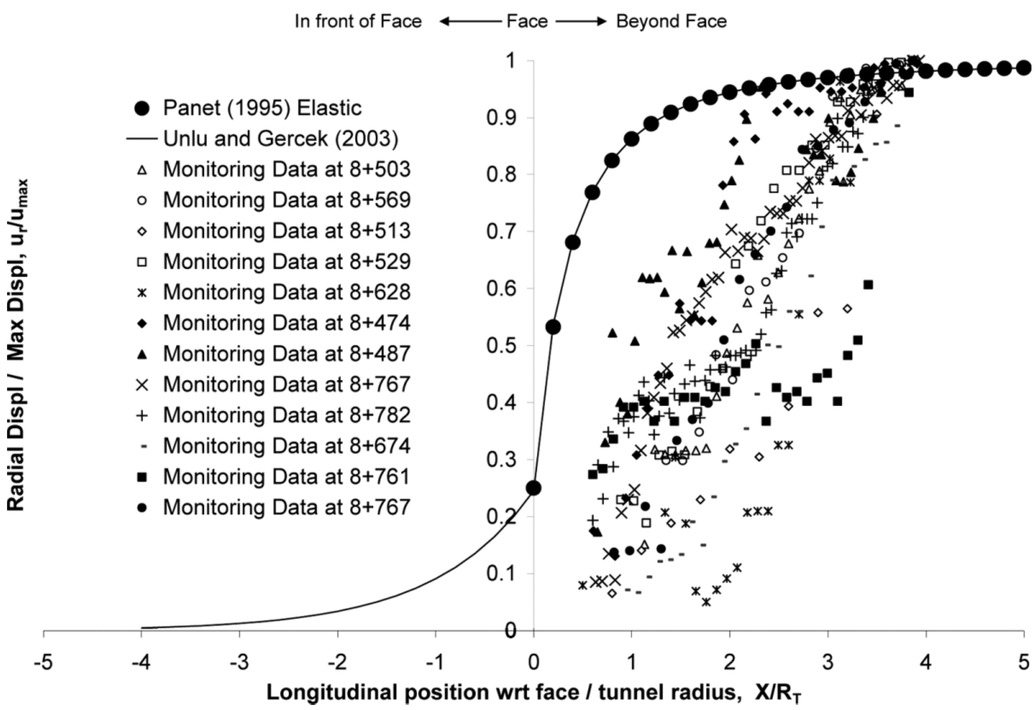

of the tunnel. One can clearly see that the accepted empirical formulations do not correlate well with the data that have been captured in the field; hence, the requirement for further investigations into this behaviour.

Based on this observation and using a series of numerical analyses, Vlachopoulos and Diederichs (2009) introduced a new series of functions defining robust LDPs, as a function of maximum normalized plastic radius. This approach takes into consideration the effect that a large ultimate plastic radius has on the rate of development of wall displacements with respect to location along the tunnel for 2D numerical analysis pseudo-capturing 3D effects. Current LDP functions (as seen in Fig. 28) are inadequate for tunnel analysis in very weak ground at great depth. This approach is valid from the elastic case through to complete plastic closure of the tunnel (as calculated using numerical or analytical solutions). Clearly, the larger and well-defined "bullet-shaped", shaded ultimate plastic zone as seen in Fig. 15 significantly influences behaviour and is not accounted for in the elastic approaches cited in Fig. 27. The larger the plastic

Fig. 29. FLAC3D model results showing the LDP for section 4.1 of staged excavation (elastic, perfectly plastic model).

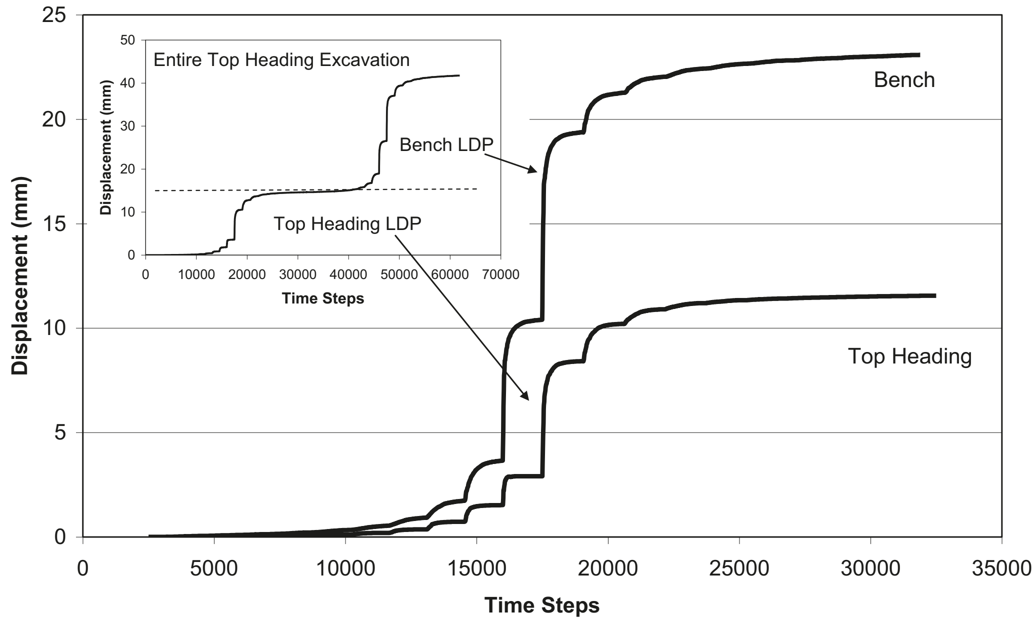

Fig. 30. Longitudinal displacement profiles associated with unsupported and supported LDPs as well as the LDPs of monitored section 4.1 of the Driskos Twin Tunnel.

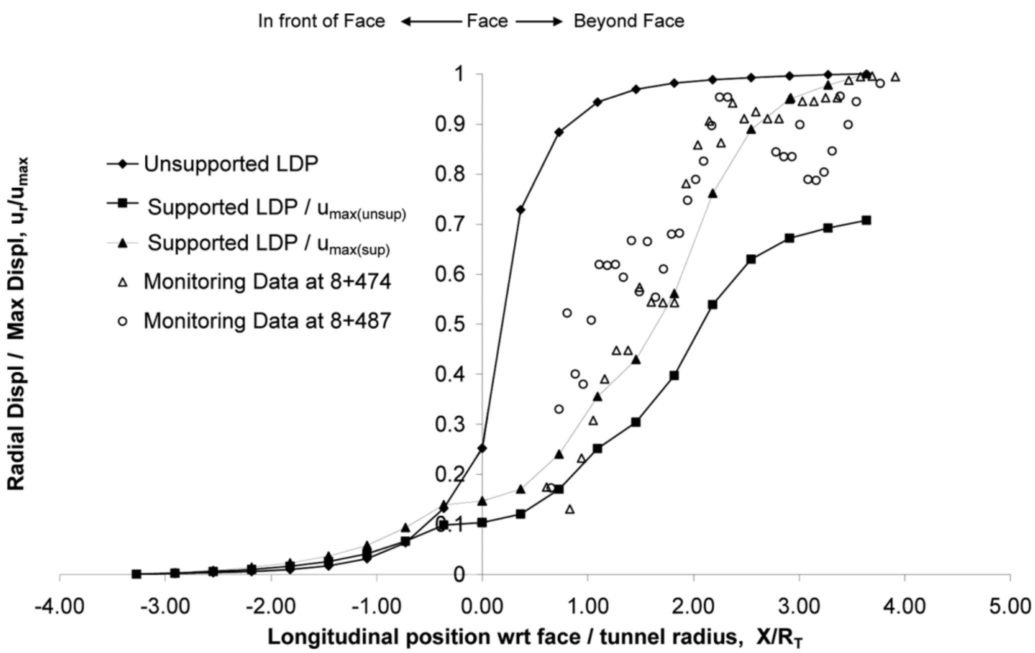

radius, the larger the expected deformations as well as the interaction with the plastic zone ahead of the tunnel face.

Another observation is that the expected behaviour in front of the face should not be expected to be the same as the behaviour past the excavation of the face. As such, LDP calculations should provide two functions: one capturing behaviour prior to the face and the other as a function of distance past the face. Continuous functions such as Panet (1995) overidealize the expected behaviour in this regard. This has also been investigated by Vlachopoulos and Diederichs (2009).

LDP selection for supported and unsupported design purposes

A legitimate question is "Which LDP does one use for design of tunnel support purposes?" The convergence–confinement method (conventional) is based on the LDP from a circular, unsupported excavation. It can be seen in Fig. 29 that if one was to plot the three-dimensionally modelled, unsupported horseshoe LDP for a staged excavation (top heading and bench), the top heading LDP and the bottom heading LDP are not similar in nature. The displacement observed for the bench LDP is approximately twice that of the top heading LDP.

It can be seen from this figure that the incremental deformation when the bench passes the point of monitoring is approximately 50% of the total additional deformation for the bench. The initial top heading, however, has incremental deformation that is approximately 25% of the total additional deformation. Clearly the same LDP cannot be used for design purposes.

Fig. 31. Longitudinal displacement profiles associated with unsupported and supported LDPs as well as the LDPs of monitored section 4.2 of the Driskos Twin Tunnel.

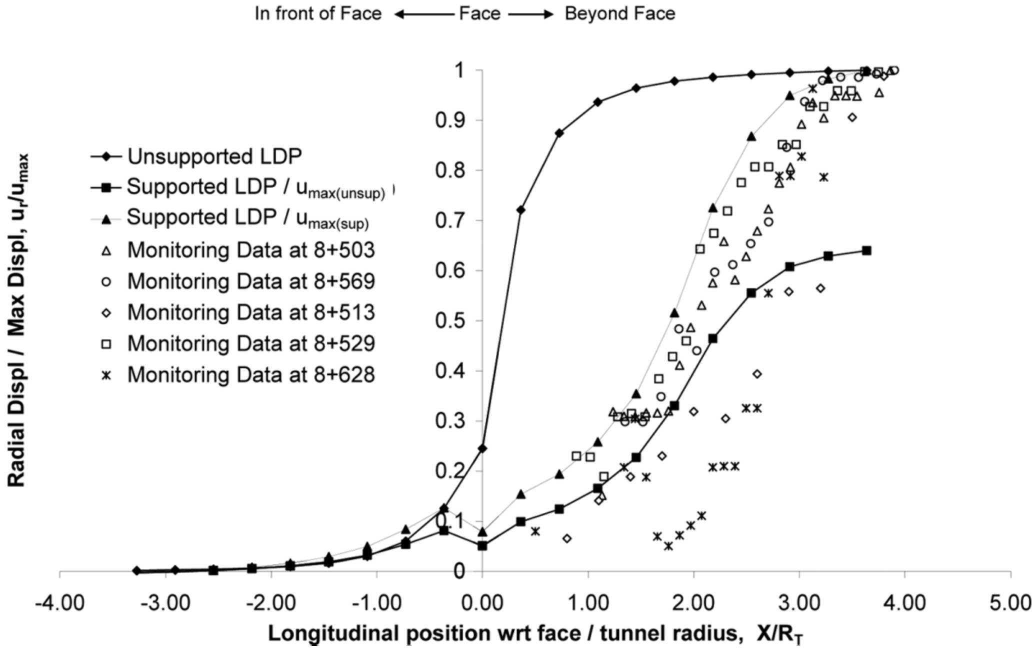

Fig. 32. Longitudinal displacement profiles associated with unsupported and supported LDPs as well as the LDPs of monitored section 4.3 of the Driskos Twin Tunnel.

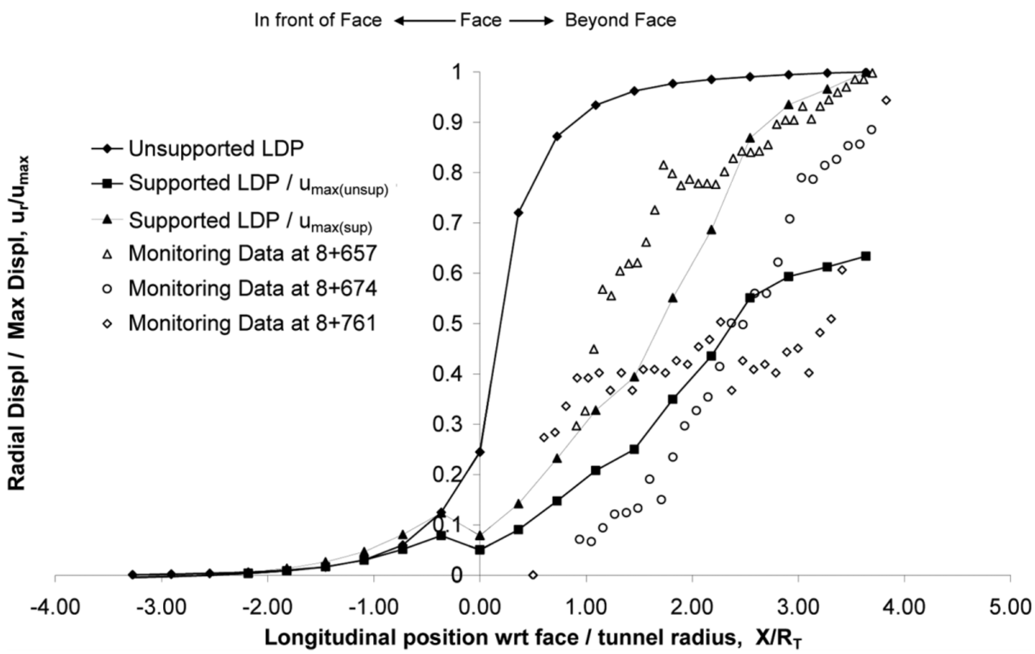

The unsupported LDP for sections 4.1 to 4.4 are shown in Figs. 30–33, respectively. Superimposed on these graphs are the FLAC3D modelled, supported LDPs normalized with respect to (*i*) the maximum supported displacement ($u_{max(sup)}$) and (*ii*) the maximum unsupported displacement ($u_{max(unsup)}$). Also included on these plots are the normalized displacements associated with the Driskos monitoring data. Chainage locations of monitoring data have been paired up with their respective sections (4.1–4.4). As can be seen, the monitoring data from Driskos track the supported LDPs well; more so the supported LDP/u_{max} supported curve.

The displacements at the face for the modelled supported runs are less than the 30% of the total displacement that were anticipated. This can be attributed to the installation of the forepole umbrella above and to 12 m in front of the face and the installation of the liner immediately after the excavation of the face that stiffens the face and provides 100% effective support to the system.

This stiffening of the face may also be attributed to the shotcrete curing rate that gains 80% of its strength within a 24 h period, well within the excavation rates for the Driskos Twin Tunnel project. The effect of the support has also been captured by the 2D Phase2 analysis shown in Fig. 34. Here, the Driskos case was simulated using an unsupported run as well as a variety of supported runs of various configurations. Highlighted here is the fact that the use of forepoles, forepoles and liner, and invert and liner (i.e., the most effective sup-

Fig. 33. Longitudinal displacement profiles associated with unsupported and supported LDPs as well as the LDPs of monitored section 4.4 of the Driskos Twin Tunnel.

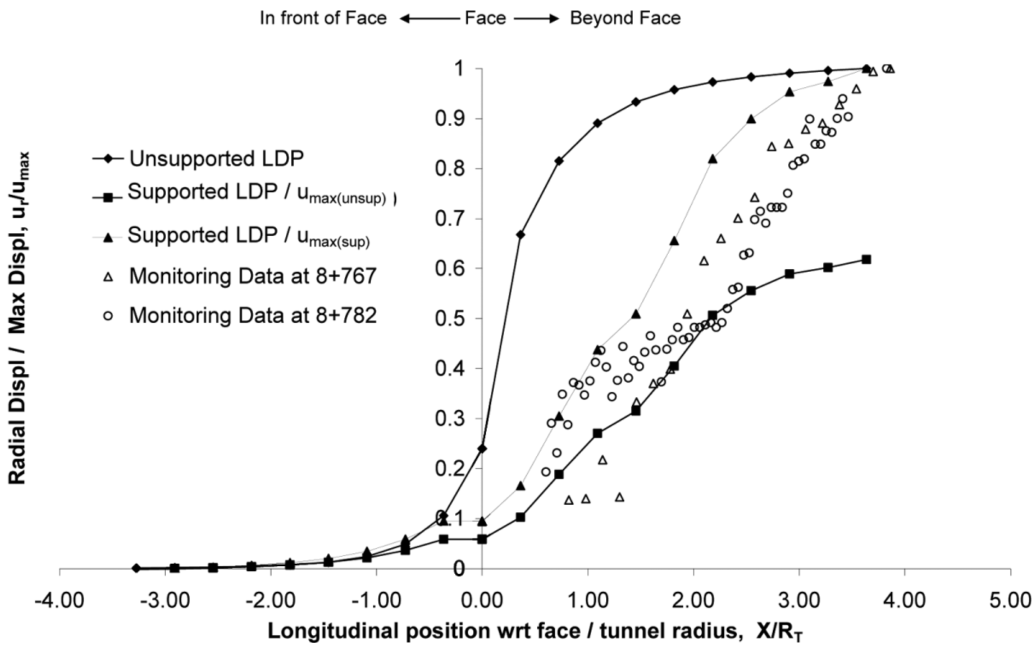

Fig. 34. Phase2 results depicting LDPs from various supported cases.

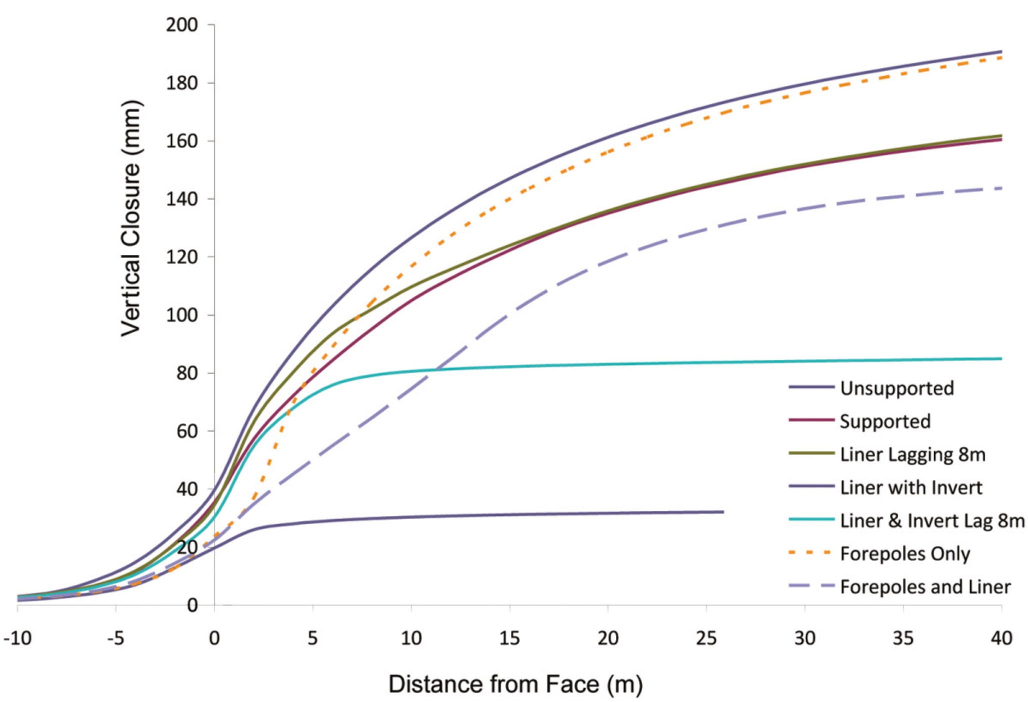

port systems controlling deformations) reduce the amount of closure ahead of and at the face. This reduction in anticipated displacements prior to and at the face is the same phenomenon that has been captured in the 3D analysis presented in Figs. 30–33.

Twin tunnel interaction

FLAC3D modelled LDPs have been plotted (Figs. 35 and 36) for the initial single tunnel that was excavated superimposed on the LDP of the twin tunnel that was excavated parallel to the initial tunnel. These were plotted for section 4.4 (weakest of the materials) and section 4.3 for the elastic, perfectly plastic constitutive model, supported and unsupported, respectively. In both cases, the LDP of the single (or first) tunnel yielded larger displacements than that of the twin (or second) tunnel. The difference is between 10% and 15% at times. As such, the FLAC3D model does not indicate much twin tunnel interaction. The monitoring data from Driskos does demonstrate an effect on the first tunnel due to excavation of the second tunnel parallel to it (Fig. 13). There are indications that a weakening or shifting of the second tunnel does occur, but this warrants further investigation.

Another interesting observation is the fact that the 3D models did not sufficiently capture the effects of the real, observed twin tunnel

Fig. 35. Relative horizontal compressive – radial closure of tunnel for elastic, perfectly plastic — supported — section 4.4 with twin tunnel.

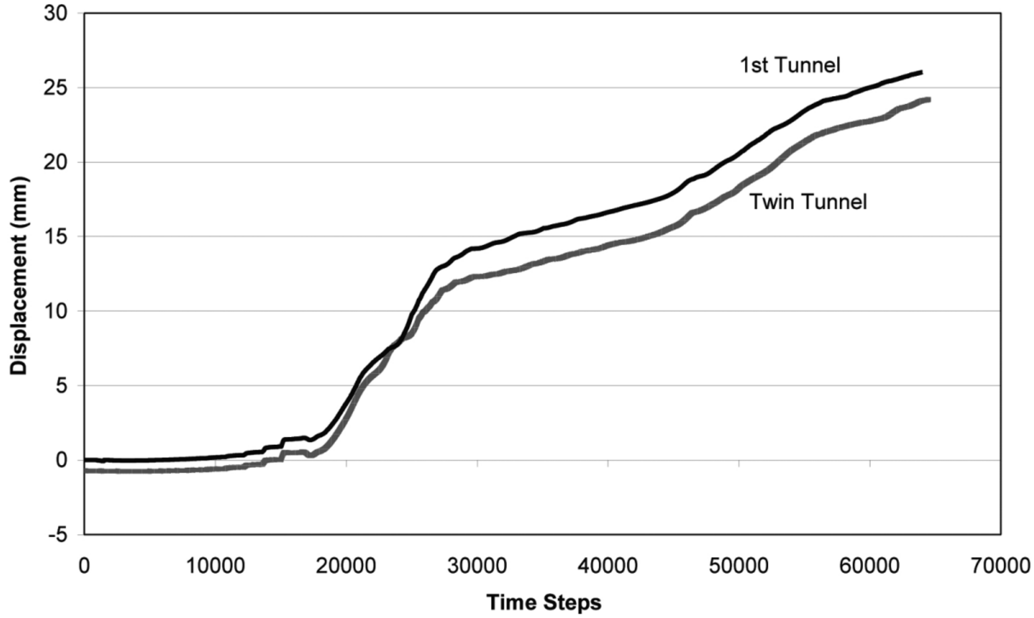

Fig. 36. Relative horizontal compressive – radial closure of tunnel for elastic, perfectly plastic — unsupported — section 4.3 with twin tunnel.

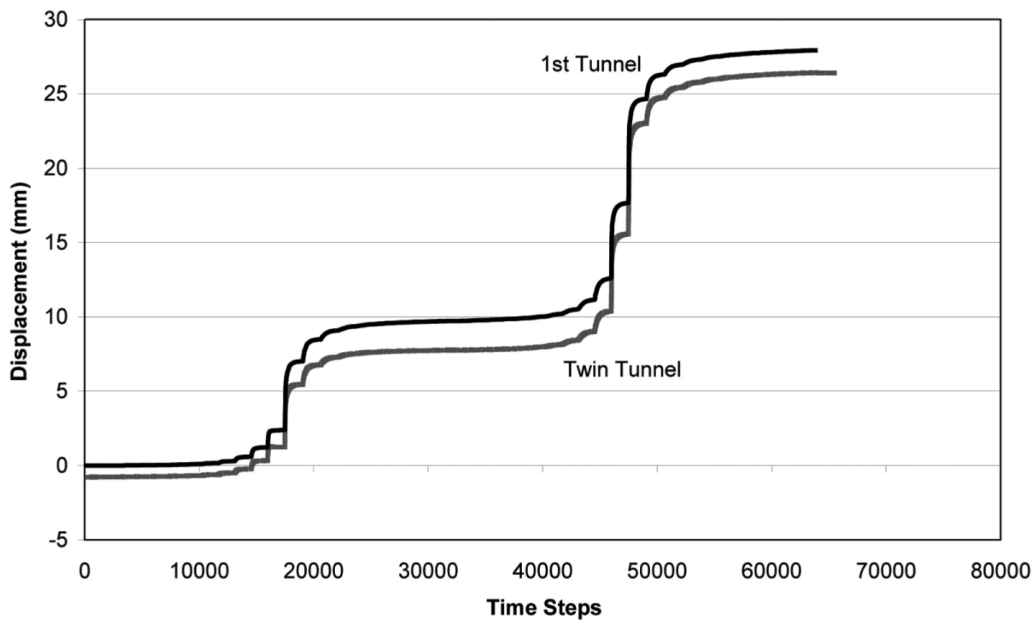

interaction in the field. In Fig. 13, the sample monitoring data from the Driskos tunneling site at chainage 8 + 503 shows that the displacements "accelerate" once the top heading of the right bore (parallel) excavation passes the face of the left bore. This can be seen in the radial closure trend Δ3. This can be attributed to the dissipation of the stresses in the longitudinal direction and not necessarily along the plane strain surface as in 2D numerical models.

GSI and effectiveness of support

In an attempt to determine that the modelled behaviour was consistent with the observed behaviour in the field, the modelled results were compared with the Driskos monitoring data. These graphs can be seen in Figs. 37–41 for material sections 4.1–4.5, respectively. The upper bound of the numerical simulations is the unsupported scenario, whereby only the rock mass behaviour is recorded (i.e., the model support is 0% effective as no support was introduced into the model). The lower bound takes into consideration the fully supported numerical model that was built to the specifications of the Driskos Twin Tunnel. This included the introduction of forepoles, rockbolts, and liner with steel sets as described previously (i.e., 100% effective model support).

As can be seen, the results of the FLAC3D model capture the monitored behaviour and trends well. The monitoring data are bound by the two extremes of 0% effective and 100% effective model support. This validates and adds confidence to the numerical model used in this investigation. Displacements predicted by the numerical model with few exceptions were in accordance with the recorded field values (Vlachopoulos 2009).

Fig. 37. Relative radial closure of Driskos Twin Tunnel for elastic, perfectly plastic supported and unsupported FLAC3D runs with Driskos monitoring data for section 4.1.

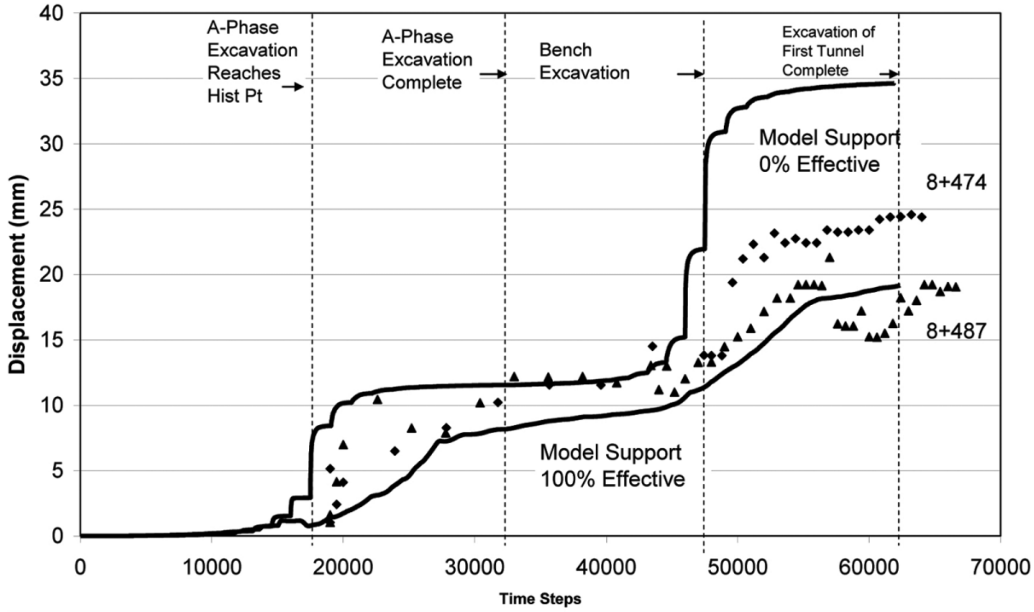

Fig. 38. Relative radial closure of Driskos Twin Tunnel for elastic, perfectly plastic supported and unsupported FLAC3D runs with Driskos monitoring data for section 4.2.

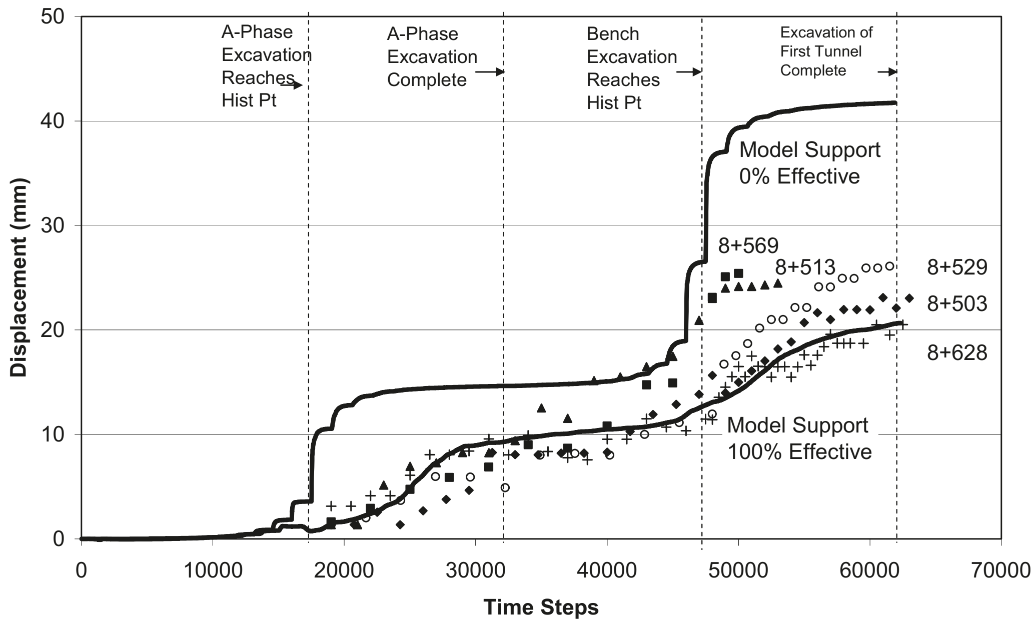

As well, the selection of GSI strength values also correlates well for each of the four sections. Illustrated in Fig. 37, however, the monitoring data at location 8 + 674 track above the upper bound of the model. This reinforces the fact that it is impossible to fully characterize all of the conditions that will be encountered during tunnel excavation over the entire length of the project. As mentioned previously, localized and unidentified (and thus unclassifiable) fault zones as well as other geological peculiarities can add to the degradation of the strength of the rock mass. The behaviour observed mimics a pattern of re-accelerated or resumed deformation often related to high tunnel convergence and failures. Excluding any measurement errors in the monitoring data (which are highly uncommon), reasons for these peculiarities can be localized ground conditions, significant changes in the local hydrological conditions (combined with the lithological effects), as well as stress transfer. Kontogianni and Stiros (2002) cites that under certain conditions high convergence is often associated with re-acceleration in the strain accumulation in neighbouring sections. This appears as steps in the strain curves. Strain may be transferred at distances >2*D* back along the tunnel outside of the zone of the face effect.

Also adding to the increase in displacements to the monitoring data during the excavation of the bench as seen in Figs. 37–40 is the radial (or system) disturbance that is caused to the upper arch system due to the installation of the “legs” of the steel sets immediately after bench excavation. This installation process

Fig. 39. Relative radial closure of Driskos Twin Tunnel for elastic, perfectly plastic supported and unsupported FLAC3D runs with Driskos monitoring data for section 4.3.

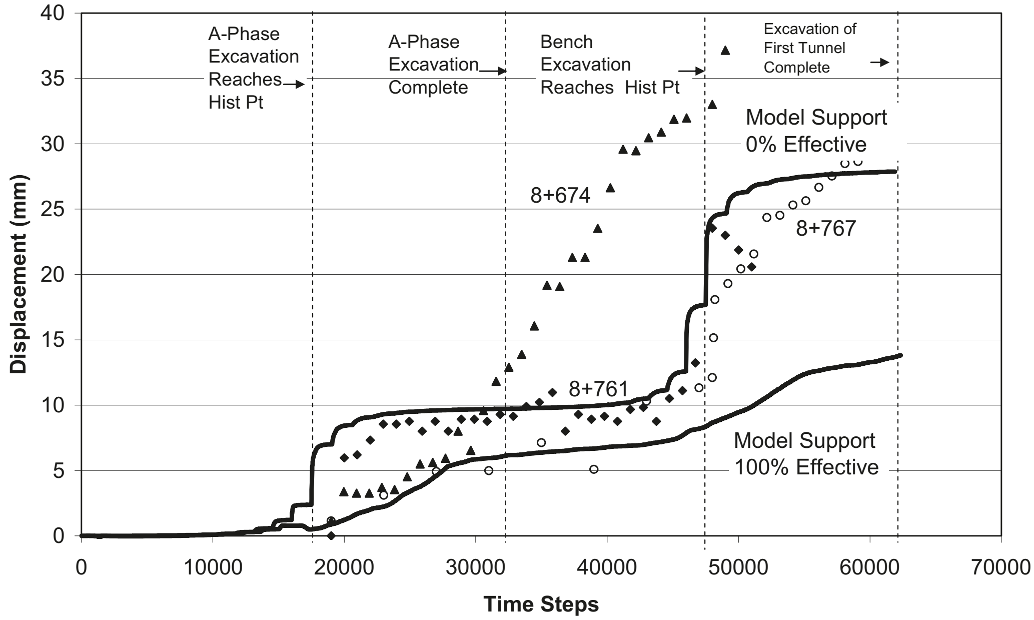

Fig. 40. Relative radial closure of Driskos Twin Tunnel for elastic, perfectly plastic supported and unsupported FLAC3D runs with Driskos monitoring data for section 4.4.

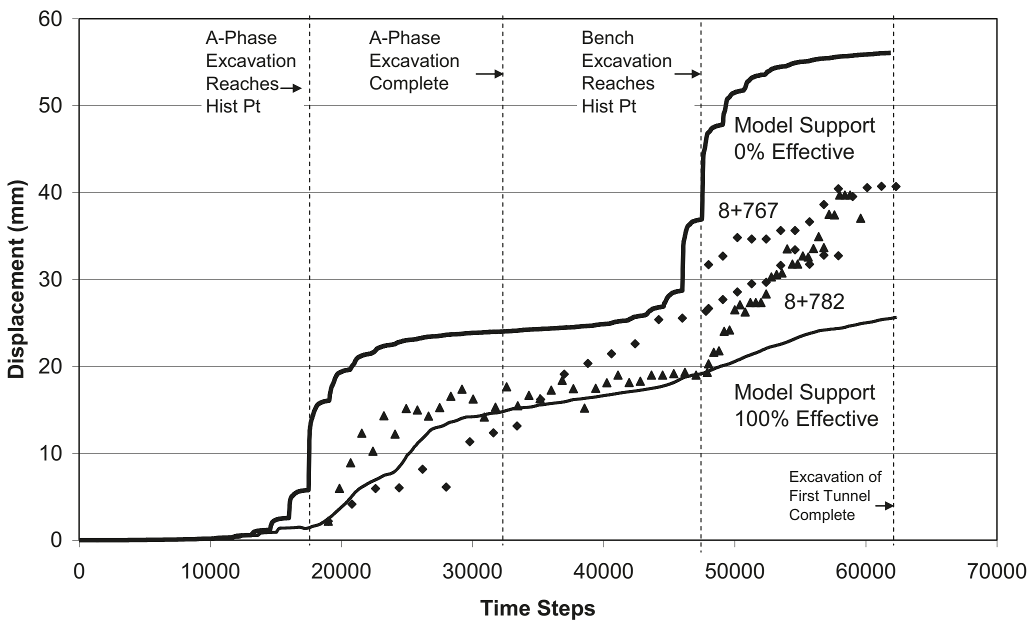

is shown in Fig. 42. Tunnelling support installation equipment cannot access the underside of the arched support without disturbing the temporary support system that has already been installed in the upper arch (top heading) region. It is important therefore to ensure a connection of limited disturbance between the top heading arched support and the arch legs. In selected designs, a shotcrete invert can be used to stabilize the top heading and assume the load that will eventually be transferred to the legs of the arch.

A bending moment diagram as extracted from the tunnel liner of the FLAC3D Driskos model for section 4.2 is seen in Fig. 43. This is a typical bending moment pattern that one would expect from such a stress environment; a symmetrical pattern of the moments about the axis of the tunnel alignment for the arched portion of the supported liner. It can also be seen that the moments approach near zero conditions where the arch portion begins and ends (positions #9 and #25). The sidewall liner connections were analyzed in conjunction with the upper arched portion to determine how stresses and moments were transferred from the arch to the support legs or struts (Fig. 44).

The moments and shears within Fig. 44 have the most extreme conditions exhibited at the connections between the arched portion and the legs (Δ0.12 MN·m for moments and Δ0.12 MN for shear). There is minimal shear transfer from the arched portion to the struts as seen in the figure. These types of connections may have to be re-assessed in terms of continuity to the arch as well as

Fig. 41. Relative radial closure of Driskos Twin Tunnel for elastic, perfectly plastic supported and unsupported FLAC3D runs with no Driskos monitoring data available for section 4.5.

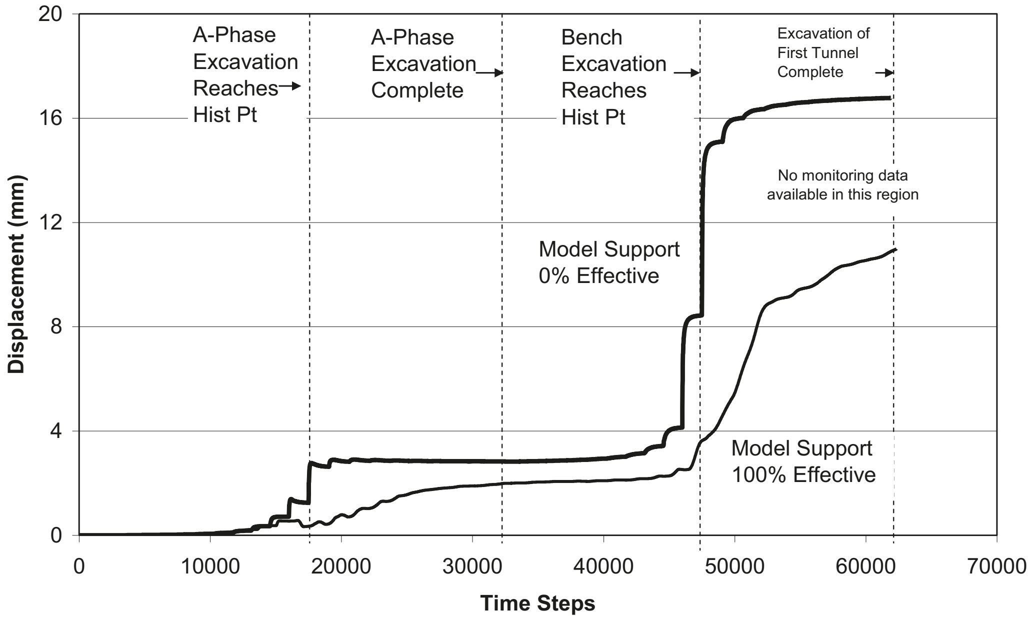

Fig. 42. Installation of steel set support in stepped excavation stages. Note that installation of the bench support cannot occur with disturbance to the existing, previously installed support (modified after Grasso et al. 2003).

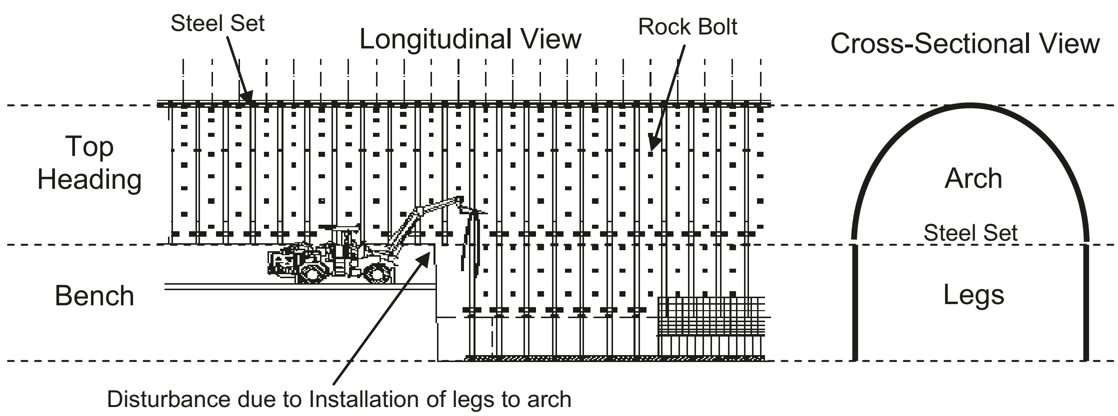

how the system is seated at the bottom of the tunnel. The arched portion, however, behaves relatively well.

The effectiveness of the support can be assessed based on a determination of the moments shears and thrusts within the liner (including whether failure has occurred). The concept of designing with the use of support capacity diagrams introduced by Kaiser (1985) and Sauer et al. (1994) can also be used to determine the effectiveness of the support system.

The support capacity diagrams take into consideration a composite lining based on shotcrete and the steel sections. Within the Driskos temporary support design, HEB 160 steel sets were used with 30 cm of shotcrete. It should be noted that the support capacity diagrams are based on elastic analysis of the composite support elements, which implies no tensile or compressive failure of the liner is acceptable. The detailed calculations of moments and forces in the lining elements has been summarized by Carranza-Torres and Diederichs (2008).

Seen in Fig. 45 are the plotted support capacity diagrams for section 4.2. It can be observed that the moment – axial thrust points for the support all fall within the capacity curves for the corresponding strength of the support with the exception of the minimal thrust outliers for a factor of safety of 1. The diagrams indicate minimum overstressing and hence, the composite lining should be reexamined and adjusted prior to proceeding to the installation of the final lining. Note that the moment thrust plots show concrete cracking (moment exceeded) only at the connection points between the arch and the struts, which is a very likely occurrence.

Conclusions

The main conclusions of the research that was undertaken are

- The behaviour of rock tunnelling of weak rock masses such as flysch can be captured accurately using continuum numerical methods (FLAC3D) of numerical analysis as Driskos Twin Tunnel data from the field correlated well with the results obtained through numerical analysis. In general the deformed flysch can be analyzed as isotropic over the tunnel scale, although heterogeneity and locally intense anisotropy can lead to inadequate support performance. The field data proved valuable in calibrating and verifying numerical models developed by the authors.
- Accurate values for GSI are difficult to obtain for extended, altering zones of weak rock masses as there are often zones whereby

Fig. 43. Bending moment diagram of liner — arched portion — for section 4.2.

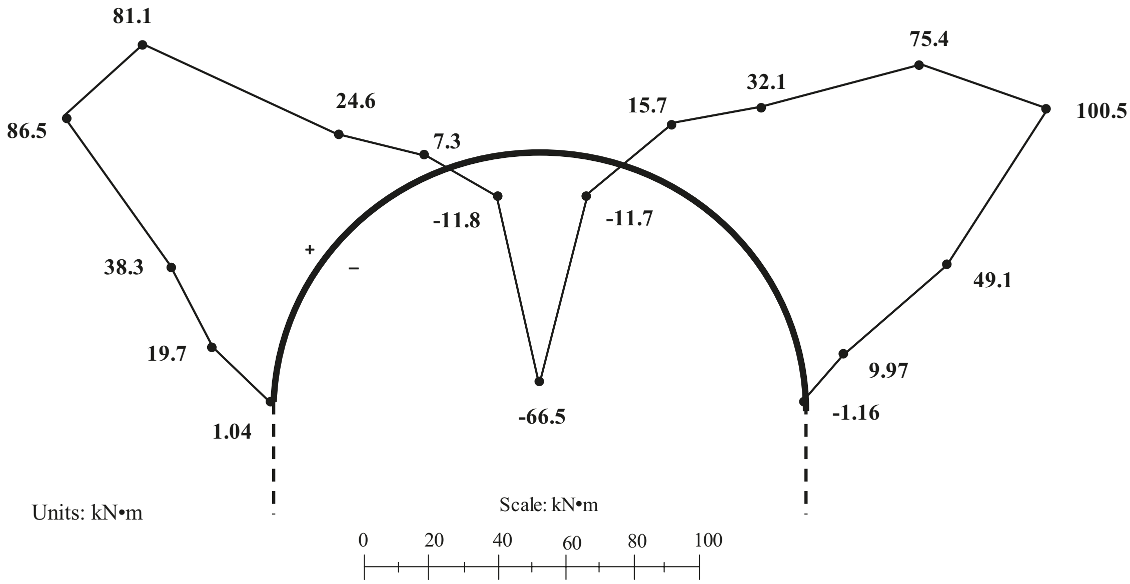

Fig. 44. Moment, shear, and thrust diagram extracted from supported liner.

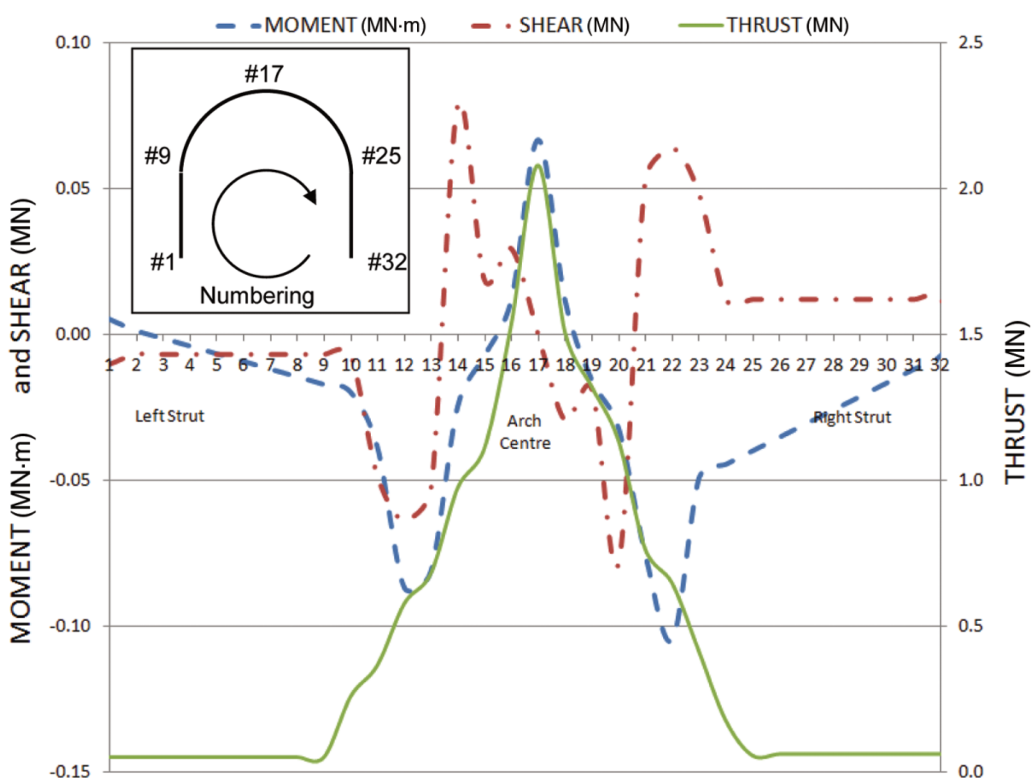

localized geological peculiarities may govern tunnel behaviour. An accurate assessment of GSI has a direct impact on input parameters for numerical modelling purposes.

- Through an assessment of the numerical modelling data, it was found that the rock mass strength calculated by Hoek (1999) correlated best to the results obtained in this investigation, rather than the same strength parameter (index value for uniaxial rock mass strength) as calculated by Hoek and Marinos 2000*a* as well as Hoek et al. 2002;
- Field data from Driskos did not correlate well with LDP equations as determined by Panet (1995), Chern et al. (1998), and Unlu and Gercek (2003). This prompted a further investigation into plastic zone development in these weak rock masses as per Vlachopoulos and Diederichs (2009).
- The LDP used for design purposes of the top heading was determined not to be the same as the LDP that was followed by the successive bench. It was found that the incremental deformation when the bench passes a certain monitoring point is approximately 50% of the total additional deformation, whereas for the initial top heading this value is approximately 25% of the total deformation. This has implications as to the selection of a proper LDP for design purposes.

Fig. 45. Support capacity diagrams for a factor of safety of 1 and 1.5 for section 4.2 of Driskos.

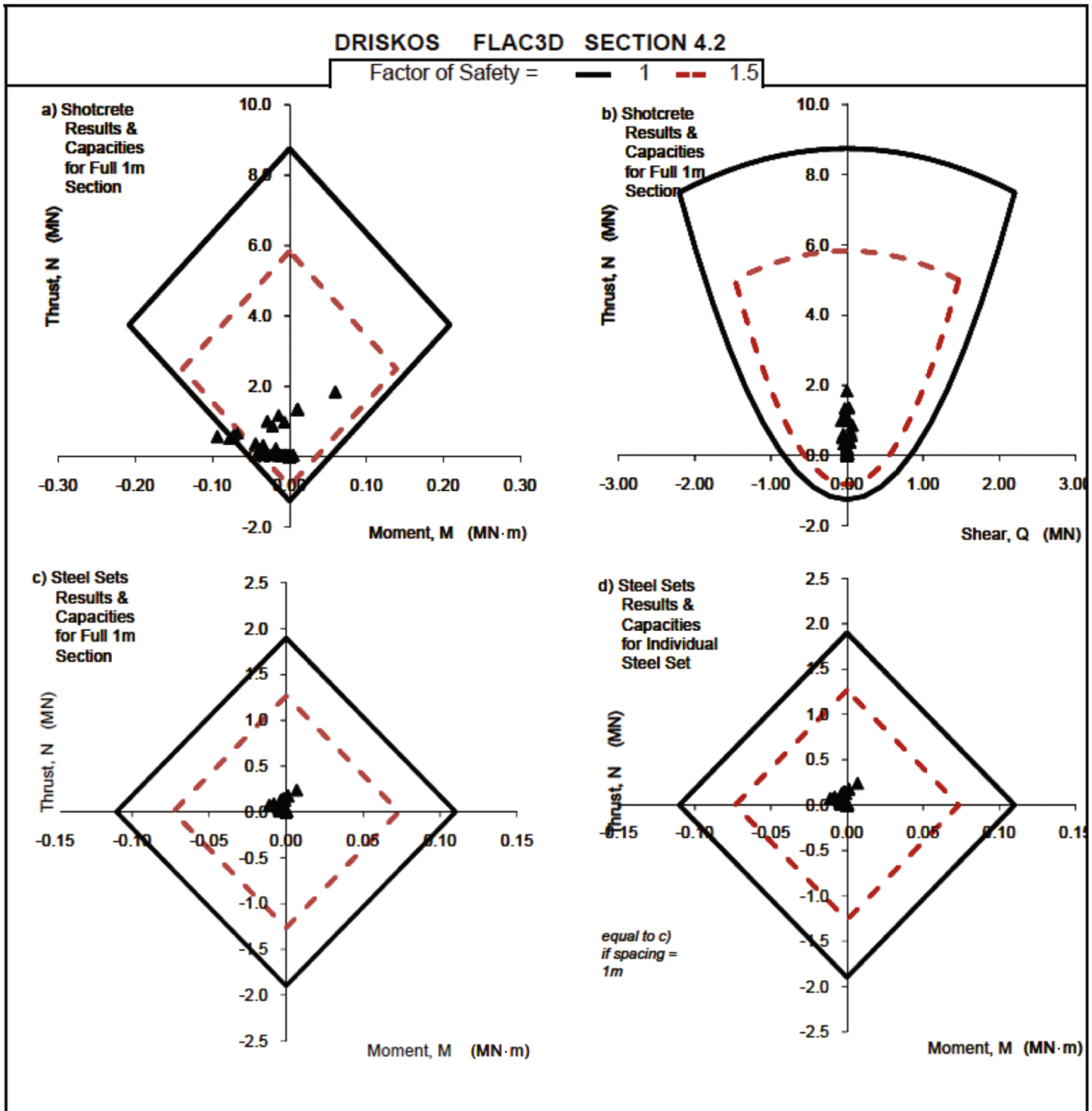

Geometry			Sets		
width of comp sect	b	1 m	height of section	ts	0.162 m
spacing btw sets	s	1 m	area of section	As	0.004748 m2
# of sets per b	n	1	moment of inertia	Is	2.231E-05 m4
			Young's Modulus	Es	200000 MPa
Shotcrete			Poisson Ratio	vs	0.25
height of section	tc	0.25 m	Comp Strength	UCSs	400 MPa
Young's Modulus	Ec	30000 MPa	Tensile Strengh	TSs	-400 MPa
Poisson Ratio	vc	0.2			
Comp Strength	UCSc	35 MPa	Equivalent Thickness	teq	0.2485926 m
Tensile Strengh	TSc	-5 MPa	Equivalent Modulus	Eeq	35501.489 MPa

- Normalized Driskos field measurements align well with the 3D modelling supported LDP normalized with the total displacement achieved by the unsupported behaviour rather than the supported LDP normalized with the total supported maximum displacement for a single tunnel bore.
- The influence of the size of the plastic zone plays a key mechanistic role within the expected deformation profile or LDP — a new series of functions has been developed to account for this influence.

Acknowledgments

Many thanks to Dr. Evert Hoek for past and future collaboration and to Egnatia Odos S.A. This work has been funded by the Natural Science and Engineering Research Council of Canada (NSERC) as well as the Province of Ontario via the PREA program.

References

Carranza-Torres, C., and Diederichs, M. 2008. Mechanical analysis of circular liners with particular reference to composite supports. For example, liners consisting of shotcrete and steel sets. Tunnelling and Underground Space Technology, **24**(5): 506–532. doi:10.1016/j.tust.2009.02.001.

Carranza-Torres, C., and Fairhurst, C. 2000. Application of the Convergence–Confinement method of tunnel design to rock masses that satisfy the Hoek–Brown failure criterion. Tunnelling and Underground Space Technology, **15**(2): 187–213. doi:10.1016/S0886-7798(00)00046-8.

Cai, M. 2008. Influence of stress path on tunnel excavation response — numerical tool selection and modeling strategy. Tunnelling and Underground Space Technology, **23**: 618–628. doi:10.1016/j.tust.2007.11.005.

Chern, J.C., Shiao, F.Y., and Yu, C.W. 1998. An empirical safety criterion for tunnel construction. *In* Proceedings of the Regional Symposium on Sedimentary Rock Engineering, Taipei, Taiwan. pp. 222–227.

Doutsos, T., Koukouvelas, I.K., and Xypolias, P. 2006. A new orogenic model for the External Hellenides. The Geological Society of London, Special Publications, **260**: 507–520. doi:10.1144/GSL.SP.2006.260.01.21.

Duncan-Fama, M.E. 1993. Numerical modeling of yield zones in weak rock. *In* Comprehensive rock engineering. *Edited by* J.A. Hudson Pergamon, Oxford. Vol. 2, pp. 49–75.

Egnatia Odos, S.A. 1998. Geological study by Asproudas and cooperates consultants. [In Greek.]

Egnatia Odos, S.A. 1999. Selection or rock mass properties for tunnel design. *In* Proceedings of the Conference on Tunnels of Egnatia Highway, Ioannina, Greece.

Egnatia Odos, S.A. 2001. The appropriate use of geological information in the design and construction of the Egnatia Motorway Tunnels, Tunnel Construction in Greece. Technical notes (MASc. program) of the National Technical University of Athens, Section 5. *Prepared by* Marinos and Hoek for Egnatia Odos, S.A.

Egnatia Odos, S.A. 2003. Evaluation of the data of the geotechnical observation of Driskos Tunnel by O.K. Consultants. [In Greek.]

Grasso, P., Scotti, G., Blasini, Pescara, M., Floria, V., and Kazilis, N. 2003. Successful application of the observational design method to difficult tunnel conditions – Driskos Tunnel, as provided by Geodata S.A.

Hindley, G., Gibbons, P., Agius, M., Carr, B., Game, R., and Kashani, K. 2004. Linking past and future. Civil Engineering Magazine, ASCE Publication, May 2004.

Hoek, E. 1999. Support for very weak rock associated with faults and shear zones. Distinguished lecture for opening of the International Symposium on Rock Support and Reinforcement Practice in Mining, Kalgoolie, Australia, 14-19 March 1999.

Hoek, E., and Brown, E.T. 1997. Practical estimates of rock mass strength. International Journal of Rock Mechanics and Mining Sciences, **34**(8): 1165–1186. doi:10.1016/S1365-1609(97)80069-X.

Hoek, E., and Diederichs, M.S. 2006. Empirical estimation of rock mass modulus. International Journal of Rock Mechanics and Mining Sciences, **43**(2): 203–215. doi:10.1016/j.ijrmms.2005.06.005.

Hoek, E., and Marinos, P. 2000*a*. Predicting squeezing problems in weak heterogeneous rock masses. Tunnels and Tunnelling International, Part 1 November 2000, Part 2 December 2000.

Hoek, E., and Marinos, P. 2000*b*. Seventh report by panel of experts (geotechnical/tunnelling) on Egnatia Odos Highway Project Sections 1.1.4, 1.1.6, 2.3, 3.2, and 11.23.

Hoek, E., and Marinos, P. 2006. Greece's Egnatia highway tunnels. Tunnels & Tunnelling International, Site Report – Greece, September 2006.

Hoek, E., Kaiser, P.K., and Bawden, W.F. 1995. Support of underground excavations in hard rock. Balkema, Rotterdam.

Hoek, E., Marinos, P., and Benissi, M. 1998. Applicability of the Geological Strength Index (GSI) classification for very weak and sheared rock masses. The case of the Athens Schist Formation. Bulletin of Engineering Geology and the Environment, **57**(2): 151–160.

Hoek, E., Carranza-Torres, C., and Corkum, B. 2002. Hoek–Brown criterion – 2002 ed. *In* Proceedings, NARMS-TAC Conference, Toronto, 2002. Vol. 1, pp. 267–273.

Itasca. 2002-2005. FLAC3D Numercial Software Package, Lagrangian Analysis of Continua. Itasca Consulting Group Inc.

Kaiser, P.K. 1985. Rational assessment of tunnel liner capacity. Proceedings of the 5th Canadian Tunnelling Conference, Montréal.

Kontogianni, V.A., and Stiros, S.C. 2002. Predictions and observations of convergence in shallow tunnels: case histories in Greece. Engineering Geology, **63**: 333–345. doi:10.1016/S0013-7952(01)00094-1.

Lunardi, P. 2000. The design and construction of tunnels using the approach based on the analysis of controlled deformation in rocks and soils. T&T International ADECO-RS Approach May 2000.

Marinos, V. 2007. Geological database of values for tunnels of Egnatia Odos. Ph.D. thesis, National Technical University of Athens.

Marinos, V. 2010. New proposed GSI classification charts for weak or complex rock masses. Bulletin of the Geological Society of Greece, Proceedings of the 12th International Congress, Patras.

Marinos, P, and Hoek, E. 2000. GSI – a geologically friendly tool for rock mass strength estimation. *In* Proceedings of GeoEng. 2000 Conference, Melbourne. pp. 1422–1442.

Marinos, P., and Hoek, E. 2001. Estimating the geotechnical properties of heterogeneous rock masses such as Flysch. Bulletin of Engineering Geology and the Environment, **60**: 85–92. doi:10.1007/s100640000090.

Marinos, V., Fortsakis, P., and Prountzopoulos, G. 2006. Estimation of rock mass properties of heavily sheared Flysch data from tunnelling construction. Geological Society Paper number 314, Pub. 22.

Marinos, P., Marinos, V., and Hoek, E. 2007. Geological Strength Index (GSI). A characterization tool for assessing engineering properties for rock masses. Underground works under special conditions. *Edited by* Romana, Perucho, Olalla. Taylor and Francis Group, London. ISBN 978-0-415-45028-7.

Panet, M. 1993. Understanding deformations in tunnels. *In* Comprehensive rock engineering, Vol. **1**. *Edited by* J.A. Hudson, E.T. Brown, C. Fairhurst, and E. Hoek Pergamon, London. pp. 663–690.

Panet, M. 1995. Calcul des tunnels par la méthode de convergence–confinement. Presses de l'Ecole Nationale des Ponts et Chaussées, Paris.

Panet, M., and Guenot, A. 1982. Analysis of convergence behind the face of a tunnel. In Proceedings, International Symposium Tunnelling'82, IMM, London. pp. 197–204.

Rocscience Inc. 2004–2007. Phase2, 2D finite element software. Available from www.rocscience.com.

Sauer, G., Gall, V., Bauer, E., and Dietmaier, P. 1994. Design of tunnel concrete linings using limit capacity curves. *In* Computer methods and advances in geomechanics. *Edited by* Siriwardane and Zaman, Rotterdam, the Netherlands. pp. 2621–2626.

Smith, M. 2000. Egnatia Highway across Northern Greece. *In* Proceedings of World Tunnelling 2000. pp. 185–190.

Structural Design, S.A. 1999. Egnatia Highway - Evaluation of the data of the geotechnical observation of Driskos Tunnel by O.K. consultants. [In Greek.]

Unlu, T., and Gercek, H. 2003. Effect of Poisson's ratio on the normalized radial displacements occurring around the face of a circular tunnel. Tunnelling and Underground Space Technology, **18**: 547–553. doi:10.1016/S0886-7798(03)00086-5.

Vlachopoulos, N. 2009. Material behaviour and near-face support issues associated with the tunneling through weak rock masses. Ph.D. thesis, Department of Geological Engineering, Queen's University, Kingston, Ont.

Vlachopoulos, N., and Diederichs, M.S. 2009. Improved longitudinal displacement profiles for convergence confinement analysis of deep tunnels. Rock Mechanics and Rock Engineering, **42**(2): 131–146. doi:10.1007/s00603-009-0176-4.